Report #06004

DIGHEM SURVEY
FOR
STRONGBOW EXPLORATION INC.
SKOONKA CREEK PROPERTY
LYTTON AREA, B.C.

NTS: 92I/5,6

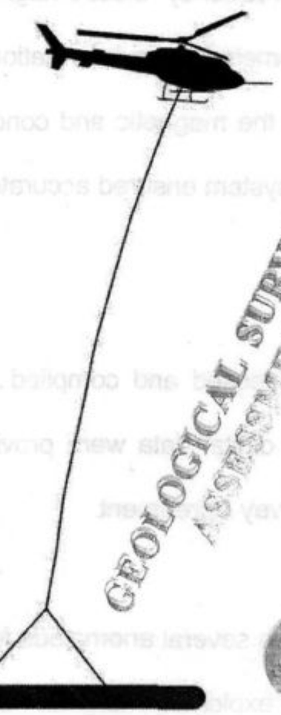

Fugro Airborne Surveys Corp.
Mississauga, Ontario

Paul A. Smith
Geophysicist

March 30, 2006

Fugro Airborne Surveys, 2270 Argentia Road, Unit 2, Mississauga, Ontario, Canada, L5N 6A6
Phone: 1 905 812 0212, Fax: 1 905 812 1504

SUMMARY

This report describes the logistics, data acquisition, processing and presentation of results of a DIGHEM airborne geophysical survey carried out for Strongbow Exploration Inc., over a property located near Lytton, British Columbia. Total coverage of the survey block amounted to 207 km. The survey was flown from January 23 to January 25, 2006.

The purpose of the survey was to detect auriferous quartz veins, to obtain a geophysical signature over known mineralized showings, and to provide information that could be used to map the geology and structure of the survey area. This was accomplished by using a DIGHEM multi-coil, multi-frequency electromagnetic system, supplemented by a high sensitivity cesium magnetometer. The information from these sensors was processed to produce maps that display the magnetic and conductive properties of the survey area. A GPS electronic navigation system ensured accurate positioning of the geophysical data with respect to the base maps.

The survey data were processed and compiled in the Fugro Airborne Surveys Toronto office. Map products and digital data were provided in accordance with the scales and formats specified in the Survey Agreement.

The survey property contains several anomalous features, a few of which are considered to be of moderate priority as exploration targets. Some of these appear to warrant further investigation using appropriate surface exploration techniques. Areas of interest may be assigned priorities on the basis of supporting geophysical, geochemical and/or geological

information. After initial investigations have been carried out, it may be necessary to re-evaluate the remaining anomalies based on information acquired from the follow-up program.

CONTENTS

APPENDICES

1. INTRODUCTION

A DIGHEM electromagnetic/resistivity/magnetic survey was flown for Strongbow Exploration Inc., from January 23 to January 25, 2006, over a survey block located about 15 km north-northeast of Lytton, British Columbia. The survey area can be located on NTS map sheet 92I/5 and 92I/6.

Survey coverage consisted of approximately 207 line-km, including 21 km of tie lines. Flight lines were flown in an azimuthal direction of 360°/180° with a line separation of 100 metres. Tie lines were flown orthogonal to the traverse lines with a line separation of 1,120 metres.

The survey employed the DIGHEM electromagnetic system. Ancillary equipment consisted of a magnetometer, radar and barometric altimeter, video camera, a digital recorder, and an electronic navigation system. The instrumentation was installed in an AS350B2 turbine helicopter (Registration C-FDNF) that was provided by Questral Helicopters Ltd. The helicopter flew at an average airspeed of 67 km/h with an EM sensor height of approximately 30 metres.

In a few portions of the survey area, the moderately steep topography forced the pilot to exceed normal terrain clearance for reasons of safety. It is possible that some weak conductors may have escaped detection in any areas where the bird height exceeded 90 m. In difficult areas where near-vertical climbs were necessary, the forward speed of the helicopter was reduced to a level that permitted excessive bird swinging. This problem, combined with the severe stresses to which the bird was subjected, gave rise to aerodynamic noise levels that are slightly higher than normal on some lines. Where warranted, reflights were carried out to minimize these adverse effects.

Figure 1: Fugro Airborne Surveys DIGHEM EM bird with AS350-B2

2. SURVEY OPERATIONS

The base of operations for the survey was established at Lytton, B.C. The survey area can be located on NTS map sheets 92I/5 and 92I/6 (Figure 2).

Table 2-1 lists the corner coordinates of the survey area in NAD83, UTM Zone 10N, central meridian 123°W.

Table 2-1

Nad83 Utm zone 10

Block	Corners	X-UTM (E)	Y-UTM (N)
06004-1	1	605000	5577500
Skoonka	2	605000	5582200
Creek, BC	3	609500	5582200
	4	609500	5578750
	5	607500	5578750
	6	607500	5577500

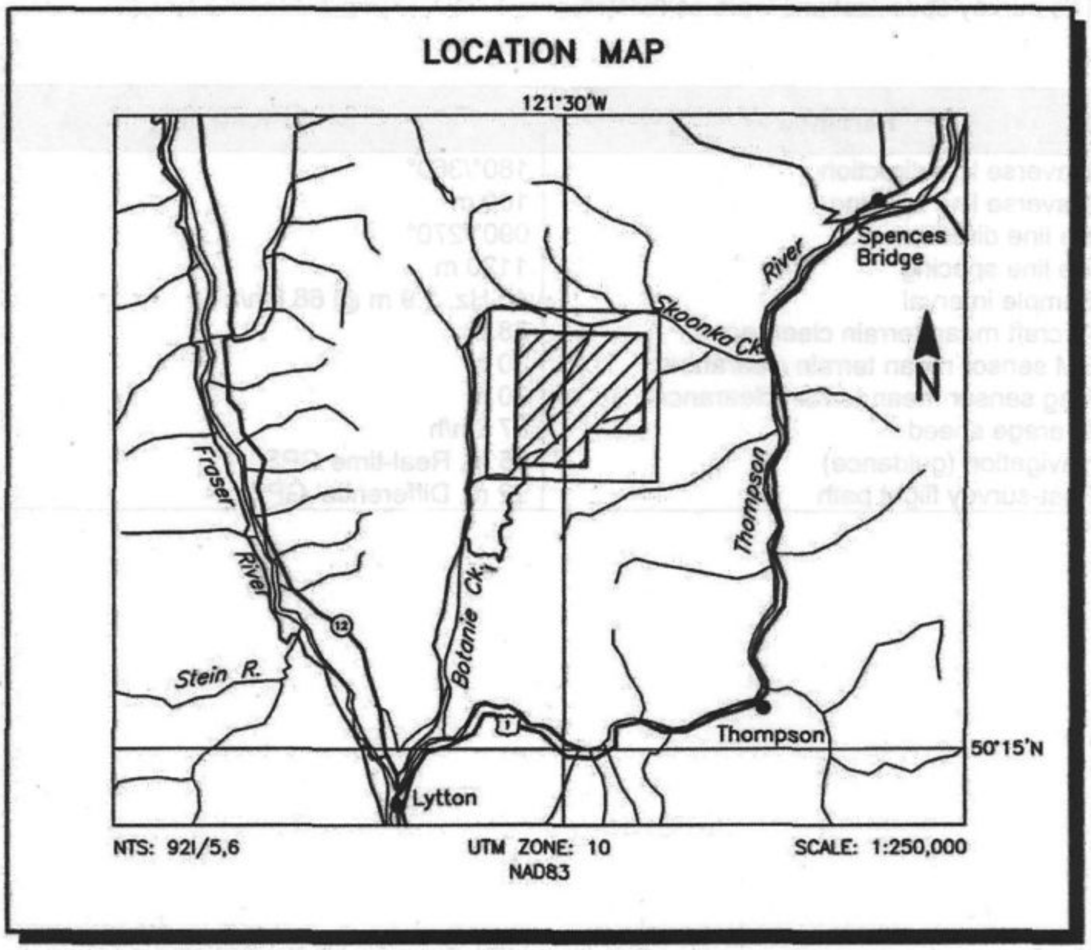

Figure 2
Location Map and Sheet Layout
Skoonka Creek Property,
Lytton, British Columbia
Job # 06004

The survey specifications were as follows:

Parameter	Specifications
Traverse line direction	180°/360°
Traverse line spacing	100 m
Tie line direction	090°/270°
Tie line spacing	1120 m
Sample interval	10 Hz, 1.9 m @ 68 km/h
Aircraft mean terrain clearance	58 m
EM sensor mean terrain clearance	30 m
Mag sensor mean terrain clearance	30 m
Average speed	67 km/h
Navigation (guidance)	±5 m, Real-time GPS
Post-survey flight path	±2 m, Differential GPS

3. SURVEY EQUIPMENT

This section provides a brief description of the geophysical instruments used to acquire the survey data and the calibration procedures employed. The geophysical equipment was installed in an AS350B2 helicopter. This aircraft provides a safe and efficient platform for surveys of this type.

Electromagnetic System

Model: DIGHEM (BKS52)

Type: Towed bird, symmetric dipole configuration operated at a nominal survey altitude of 30 metres. Coil separation is 8 metres for 900 Hz, 1000 Hz, 5500 Hz and 7200 Hz, and 6.3 metres for the 56,000 Hz coil-pair.

Coil orientations, frequencies and dipole moments

Atm^2	orientation	nominal	actual
211	coaxial	/ 1000 Hz	1112 Hz
211	coplanar	/ 900 Hz	870 Hz
67	coaxial	/ 5500 Hz	5687 Hz
56	coplanar	/ 7200 Hz	7298 Hz
15	coplanar	/ 56,000 Hz	55,400 Hz

Channels recorded:
5 in-phase channels
5 quadrature channels
2 monitor channels

Sensitivity:
0.06 ppm at 1000 Hz Cx
0.12 ppm at 900 Hz Cp
0.12 ppm at 5,500 Hz Cx
0.24 ppm at 7,200 Hz Cp
0.60 ppm at 56,000 Hz Cp

Sample rate: 10 per second, equivalent to 1 sample every 1.8 m, at a survey speed of 68 km/h.

The electromagnetic system utilizes a multi-coil coaxial/coplanar technique to energize conductors in different directions. The coaxial coils are vertical with their axes in the flight direction. The coplanar coils are horizontal. The secondary fields are sensed simultaneously by means of receiver coils that are maximum coupled to their respective transmitter coils. The system yields an in-phase and a quadrature channel from each transmitter-receiver coil-pair.

In-Flight EM System Calibration

Calibration of the system during the survey uses the Fugro AutoCal automatic, internal calibration process. At the beginning and end of each flight, and at intervals during the flight, the system is flown up to high altitude to remove it from any "ground effect" (response from the earth). Any remaining signal from the receiver coils (base level) is measured as the zero level, and is removed from the data collected until the time of the next calibration. Following the zero level setting, internal calibration coils, for which the response phase and amplitude have been determined at the factory, are automatically triggered – one for each frequency. The on-time of the coils is sufficient to determine an accurate response through any ambient noise. The receiver response to each calibration coil "event" is compared to the expected response (from the factory calibration) for both phase angle and amplitude, and any phase and gain corrections are automatically applied to bring the data to the correct value.

In addition, the outputs of the transmitter coils are continuously monitored during the survey, and the gains are adjusted to correct for any change in transmitter output.

Because the internal calibration coils are calibrated at the factory (on a resistive halfspace) ground calibrations using external calibration coils on-site are not necessary for system calibration. A check calibration may be carried out on-site to ensure all systems are working correctly. All system calibrations will be carried out in the air, at sufficient altitude that there will be no measurable response from the ground.

The internal calibration coils are rigidly positioned and mounted in the system relative to the transmitter and receiver coils. In addition, when the internal calibration coils are calibrated at the factory, a rigid jig is employed to ensure accurate response from the external coils.

Using real time Fast Fourier Transforms and the calibration procedures outlined above, the data are processed in real time, from measured total field at a high sampling rate, to in-phase and quadrature values at 10 samples per second.

Airborne Magnetometer

Model:	Fugro D1344 processor with Scintrex CS2 sensor
Type:	Optically pumped cesium vapour
Sensitivity:	0.01 nT
Sample rate:	10 per second

The magnetometer sensor is housed in the EM bird, 28 m below the helicopter.

Magnetic Base Station

Primary

Model:	Fugro CF1 base station with timing provided by integrated GPS	
Sensor type:	Scintrex CS-2	
Counter specifications:	Accuracy:	±0.1 nT
	Resolution:	0.01 nT
	Sample rate	1 Hz
GPS specifications:	Model:	Marconi Allstar
	Type:	Code and carrier tracking of L1 band, 12-channel, C/A code at 1575.42 MHz
	Sensitivity:	-90 dBm, 1.0 second update
	Accuracy:	Manufacturer's stated accuracy for differential corrected GPS is 2 metres

Environmental Monitor specifications: Temperature:

- Accuracy: ±1.5°C max
- Resolution: 0.0305°C
- Sample rate: 1 Hz
- Range: -40°C to +75°C

Barometric pressure:

- Model: Motorola MPXA4115A
- Accuracy: ±3.0° kPa max (-20°C to 105°C temp. ranges)
- Resolution: 0.013 kPa
- Sample rate: 1 Hz
- Range: 55 kPa to 108 kPa

<u>Backup</u>

Model:	GEM Systems GSM-19T
Type:	Digital recording proton precession
Sensitivity:	0.10 nT
Sample rate:	3 second intervals

A digital recorder is operated in conjunction with the base station magnetometer to record the diurnal variations of the earth's magnetic field. The clock of the base station is synchronized with that of the airborne system, using GPS time, to permit subsequent removal of diurnal drift. The Fugro CF1 was the primary magnetic base station. It was located at Lytton at Lat. 50°14'31.66"N, Long. 120°31'14.94"W, at an ellipsoidal elevation of 260 m. The second back-up unit was set up at the Lytton airport.

Navigation (Global Positioning System)

<u>Airborne Receiver for Real-time Navigation & Guidance</u>

Model:	Ashtech Z-Surveyor
Type:	Code and carrier tracking of L1 band, 12-channel, dual frequency C/A code at 1575.2 MHz, and L2 P-code 1227 MHz.
Sample rate:	0.5 second update.

Accuracy: Manufacturer's stated accuracy for differential corrected GPS is better than 1 metre.

Antenna: Mounted on tail of helicopter.

Primary Base Station for Post-Survey Differential Correction

Model: Novatel Millennium.

Type: Code and carrier tracking of L1-C/A code at 1575.42 MHz and L2-P code at 1227.0 MHz. Dual frequency, 24-channel.

Sample rate: 10 Hz update.

Accuracy: Better than 1 metre in differential mode.

Secondary GPS Base Station

Model: Marconi Allstar OEM, CMT-1200

Type: Code and carrier tracking of L1 band, 12-channel, C/A code at 1575.42 MHz

Sensitivity: -90 dBm, 1.0 second update

Accuracy: Manufacturer's stated accuracy for differential corrected GPS is 2 metres.

The Ashtech Z-Surveyor is a line of sight, satellite navigation system that utilizes time-coded signals from at least four of forty-eight available satellites. The satellite constellations are used to calculate the position and to provide real time guidance to the helicopter. For flight path processing a Novatel Millennium was used as the primary base station receiver. The mobile and base station raw XYZ data were recorded, thereby permitting post-survey differential corrections for theoretical accuracies of better than 2 metres. A Marconi Allstar GPS unit, part of the CF-1, was used as a secondary (back-up) base station.

The base station receiver is able to calculate its own latitude and longitude. For this survey, the primary GPS station was located at Lytton Airport, at latitude 50°14'13.71"N, longitude 121°34'15.49"W at an elevation of 274 metres above the ellipsoid. The secondary GPS unit was located at the coordinates given for the CFI base station. The GPS records data relative to the WGS84 ellipsoid, which is the basis of the revised North American Datum (NAD83). Conversion software is used to transform the WGS84 coordinates to the NAD83 UTM system displayed on the maps.

Radar Altimeter

Manufacturer:	Honeywell/Sperry
Model:	RT300
Type:	Short pulse modulation, 4.3 GHz
Sensitivity:	0.3 m
Sample rate:	2 per second

The radar altimeter measures the vertical distance between the helicopter and the ground. This information is used in the processing algorithm that determines conductor depth.

Barometric Pressure and Temperature Sensors

Model:	DIGHEM D 1300
Type:	Motorola MPX4115AP analog pressure sensor AD592AN high-impedance remote temperature sensors
Sensitivity:	Pressure: 150 mV/kPa Temperature: 100 mV/°C or 10 mV/°C (selectable)
Sample rate:	10 per second

The D1300 circuit is used in conjunction with one barometric sensor and up to three temperature sensors. Two sensors (baro and temp) are installed in the EM console in the aircraft, to monitor pressure (1KPA) and internal operating temperatures (2TDC). A third sensor (3TDC) is located in the bird, to monitor ambient operating temperatures.

Digital Data Acquisition System

Manufacturer:	Fugro
Model:	Helidas
Recorder:	IBM Microdrive

The stored data are downloaded to the field workstation PC at the survey base, for verification, backup and preparation of in-field products.

Video Flight Path Recording System

Type:	Panasonic WVCL322 Colour Video Camera
Recorder:	Panasonic AG 2400
Format:	NTSC (VHS)

Fiducial numbers are recorded continuously and are displayed on the margin of each image. This procedure ensures accurate correlation of data with respect to visible features on the ground.

4. QUALITY CONTROL AND IN-FIELD PROCESSING

Digital data for each flight were transferred to the field workstation, in order to verify data quality and completeness. A database was created and updated using Geosoft Oasis Montaj and proprietary Fugro Atlas software. This allowed the field personnel to calculate, display and verify both the positional (flight path) and geophysical data on a screen or printer. Records were examined as a preliminary assessment of the data acquired for each flight.

In-field processing of Fugro survey data consists of differential corrections to the airborne GPS data, verification of EM calibrations, drift correction of the raw airborne EM data, spike rejection and filtering of all geophysical and ancillary data, verification of flight videos, calculation of preliminary resistivity data, diurnal correction, and preliminary leveling of magnetic data.

All data, including base station records, were checked on a daily basis, to ensure compliance with the survey contract specifications. Reflights were required if any of the following specifications were not met.

Navigation - Positional (x,y) accuracy of better than 10 m, with a CEP (circular error of probability) of 95%.

Flight Path - No lines to exceed ±25% departure from nominal line spacing over a continuous distance of more than 1 km, except for reasons of safety.

Clearance - Mean terrain sensor clearance of 30 m, ±10 m, except where precluded by safety considerations, e.g., restricted or populated areas, severe topography, obstructions, tree canopy, aerodynamic limitations, etc.

Airborne Mag - Aerodynamic magnetometer noise envelope not to exceed 0.5 nT and the non-normalized 4^{th} difference not to exceed 1.6 nT over a distance of more than 1 km.

Base Mag - Diurnal variations not to exceed 10 nT over a straight line time chord of 1 minute.

EM - Spheric pulses may occur having strong peaks but narrow widths. The EM data area considered acceptable when their occurrence is less than 10 spheric events exceeding the stated noise specification for a given frequency per 100 samples continuously over a distance of 2,000 metres.

Frequency	Coil Orientation	Peak to Peak Noise Envelope (ppm)
1000 Hz	horizontal coaxial	5.0
900 Hz	horizontal coplanar	10.0
5500 Hz	vertical coaxial	10.0
7200 Hz	horizontal coplanar	20.0
56,000 Hz	horizontal coplanar	40.0

5. DATA PROCESSING

Flight Path Recovery

The raw range data from at least four satellites are simultaneously recorded by both the base and mobile GPS units. The geographic positions of both units, relative to the model ellipsoid, are calculated from this information. Differential corrections, which are obtained from the base station, are applied to the mobile unit data to provide a post-flight track of the aircraft, accurate to within 2 m. Speed checks of the flight path are also carried out to determine if there are any spikes or gaps in the data.

The corrected WGS84 latitude/longitude coordinates are transformed to the NAD83 UTM coordinate system used on the final maps. Images or plots are then created to provide a visual check of the flight path.

Electromagnetic Data

EM data are processed at the recorded sample rate of 10 samples/second. Spheric rejection median and Hanning filters are then applied to reduce noise to acceptable levels. EM test profiles are then created to allow the interpreter to select the most appropriate EM anomaly picking controls for a given survey area. The EM picking parameters depend on several factors but are primarily based on the dynamic range of the resistivities within the survey area, and the types and expected geophysical responses of the targets being sought.

Anomalous electromagnetic responses are selected and analysed by computer to provide a preliminary electromagnetic anomaly map. The automatic selection algorithm is intentionally oversensitive to assure that no meaningful responses are missed. Using the preliminary map in conjunction with the multi-parameter stacked profiles, the interpreter then classifies the anomalies according to their source and eliminates those that are not substantiated by the data. The final interpreted EM anomaly map includes bedrock, surficial and cultural conductors. A map containing only bedrock conductors can be generated, if desired.

Apparent Resistivity

The apparent resistivities in ohm-m are generated from the in-phase and quadrature EM components for all of the coplanar frequencies, using a pseudo-layer half-space model. The inputs to the resistivity algorithm are the in-phase and quadrature amplitudes of the secondary field. The algorithm calculates the apparent resistivity in ohm-m, and the apparent height of the bird above the conductive source. Any difference between the apparent height and the true height, as measured by the radar altimeter, is called the pseudo-layer and reflects the difference between the real geology and a homogeneous halfspace. This difference is often attributed to the presence of a highly resistive upper layer. Any errors in the altimeter reading, caused by heavy tree cover, are included in the pseudo-layer and do not affect the resistivity calculation. The apparent depth estimates, however, will reflect the altimeter errors. Apparent resistivities calculated in this manner may differ from those calculated using other models.

In areas where the effects of magnetic permeability or dielectric permittivity have suppressed the in-phase responses, the calculated resistivities will be erroneously high. Various algorithms and inversion techniques can be used to partially correct for the effects of permeability and permittivity.

Apparent resistivity maps portray all of the information for a given frequency over the entire survey area. This full coverage contrasts with the electromagnetic anomaly map, which provides information only over interpreted conductors. The large dynamic range afforded by the multiple frequencies makes the apparent resistivity parameter an excellent mapping tool.

The preliminary apparent resistivity maps and images are carefully inspected to identify any lines or line segments that might require base level adjustments. Subtle changes between in-flight calibrations of the system can result in line-to-line differences that are more recognizable in resistive (low signal amplitude) areas. If required, manual level adjustments are carried out to eliminate or minimize resistivity differences that can be attributed, in part, to changes in operating temperatures. These leveling adjustments are usually very subtle, and do not result in the degradation of discrete anomalies.

After the manual leveling process is complete, revised resistivity grids are created. The resulting grids can be subjected to a microleveling technique in order to smooth the data for contouring. The coplanar resistivity parameter has a broad 'footprint' that requires very little filtering.

The calculated resistivities for the 900 Hz, 7200 Hz, and 56,000 Hz coplanar frequencies are included in the XYZ and grid archives. Values are in ohm-metres on all final products.

Dielectric Permittivity and Magnetic Permeability Corrections[1]

In resistive areas having magnetic rocks, the magnetic and dielectric effects will both generally be present in high-frequency EM data, whereas only the magnetic effect will exist in low-frequency data.

The magnetic permeability is first obtained from the EM data at the lowest frequency, because the ratio of the magnetic response to conductive response is maximized and because displacement currents are negligible. The homogeneous half-space model is used. The computed magnetic permeability is then used along with the in-phase and quadrature response at the highest frequency to obtain the relative dielectric permittivity, again using the homogeneous half-space model. The highest frequency is used because the ratio of dielectric response to conductive response is maximized. The resistivity can then be determined from the measured in-phase and quadrature components of each frequency, given the relative magnetic permeability and relative dielectric permittivity.

---

[1] Huang, H. and Fraser, D.C., 2001 Mapping of the Resistivity, Susceptibility, and Permittivity of the Earth Using a Helicopter-borne Electromagnetic System: Geophysics 106 pg 148-157.

Resistivity-depth Sections (optional)

The apparent resistivities for all frequencies can be displayed simultaneously as coloured resistivity-depth sections. Usually, only the coplanar data are displayed as the close frequency separation between the coplanar and adjacent coaxial data tends to distort the section. The sections can be plotted using the topographic elevation profile as the surface. The digital terrain values, in metres a.m.s.l., can be calculated from the GPS Z-value or barometric altimeter, minus the aircraft radar altimeter.

Resistivity-depth sections can be generated in three formats:

(1) Sengpiel resistivity sections, where the apparent resistivity for each frequency is plotted at the depth of the centroid of the in-phase current flow[2]; and,

(2) Differential resistivity sections, where the differential resistivity is plotted at the differential depth[3].

(3) Occam[4] or Multi-layer[5] inversion.

---

2 Sengpiel, K.P., 1988, Approximate Inversion of Airborne EM Data from Multilayered Ground: Geophysical Prospecting 36, 446-459.

3 Huang, H. and Fraser, D.C., 1993, Differential Resistivity Method for Multi-frequency Airborne EM Sounding: presented at Intern. Airb. EM Workshop, Tucson, Ariz.

4 Constable et al, 1987, Occam's inversion: a practical algorithm for generating smooth models from electromagnetic sounding data: Geophysics, 52, 289-300.

5 Huang H., and Palacky, G.J., 1991, Damped least-squares inversion of time domain airborne EM data based on singular value decomposition: Geophysical Prospecting, 39, 827-844.

Both the Sengpiel and differential methods are derived from the pseudo-layer half-space model. Both yield a coloured resistivity-depth section that attempts to portray a smoothed approximation of the true resistivity distribution with depth. Resistivity-depth sections are most useful in conductive layered situations, but may be unreliable in areas of moderate to high resistivity where signal amplitudes are weak. In areas where in-phase responses have been suppressed by the effects of magnetite, or adversely affected by cultural features, the computed resistivities shown on the sections may be unreliable.

Both the Occam and multi-layer inversions compute the layered earth resistivity model that would best match the measured EM data. The Occam inversion uses a series of thin, fixed layers (usually 20 x 5m and 10 x 10m layers) and computes resistivities to fit the EM data. The multi-layer inversion computes the resistivity and thickness for each of a defined number of layers (typically 3-5 layers) to best fit the data.

Total Magnetic Field

A fourth difference editing routine was applied to the magnetic data to remove any spikes. The aeromagnetic data were corrected for diurnal variation using the magnetic base station data. The results were then leveled using tie and traverse line intercepts. Manual adjustments were applied to any lines that required leveling, as indicated by shadowed images of the gridded magnetic data. The manually leveled data were then subjected to a microleveling filter.

Calculated Vertical Magnetic Gradient

The diurnally-corrected total magnetic field data were subjected to a processing algorithm that enhances the response of magnetic bodies in the upper 500 m and attenuates the response of deeper bodies. The resulting vertical gradient map provides better definition and resolution of near-surface magnetic units. It also identifies weak magnetic features that may not be evident on the total field map. However, regional magnetic variations and changes in lithology may be better defined on the total magnetic field map.

EM Magnetite (optional)

The apparent percent magnetite by weight is computed wherever magnetite produces a negative in-phase EM response. This calculation is more meaningful in resistive areas.

Magnetic Derivatives (optional)

The total magnetic field data can be subjected to a variety of filtering techniques to yield maps or images of the following:

- enhanced magnetics
- second vertical derivative
- reduction to the pole/equator
- magnetic susceptibility with reduction to the pole

upward/downward continuations

analytic signal

All of these filtering techniques improve the recognition of near-surface magnetic bodies, with the exception of upward continuation. Any of these parameters can be produced on request.

Digital Elevation (optional)

The radar altimeter values (ALTR – aircraft to ground clearance) are subtracted from the differentially corrected and de-spiked GPS-Z values to produce profiles of the height above the ellipsoid along the survey lines. These values are gridded to produce contour maps showing approximate elevations within the survey area. The calculated digital terrain data are then tie-line leveled and adjusted to mean sea level. Any remaining subtle line-to-line discrepancies are manually removed. After the manual corrections are applied, the digital terrain data are filtered with a microleveling algorithm.

The accuracy of the elevation calculation is directly dependent on the accuracy of the two input parameters, ALTR and GPS-Z. The ALTR value may be erroneous in areas of heavy tree cover, where the altimeter reflects the distance to the tree canopy rather than the ground. The GPS-Z value is primarily dependent on the number of available satellites. Although post-processing of GPS data will yield X and Y accuracies in the order of 1-2 metres, the accuracy of the Z value is usually much less, sometimes in the

±10 metre range. Further inaccuracies may be introduced during the interpolation and gridding process.

Because of the inherent inaccuracies of this method, no guarantee is made or implied that the information displayed is a true representation of the height above sea level. Although this product may be of some use as a general reference, THIS PRODUCT MUST NOT BE USED FOR NAVIGATION PURPOSES.

Contour, Colour and Shadow Map Displays

The geophysical data are interpolated onto a regular grid using a modified Akima spline technique. The resulting grid is suitable for image processing and generation of contour maps. The grid cell size was 20% of the line interval for the magnetic and resistivity grids. The radiometric grids were created using a minimum curvature technique with a cell size of 33% of the line interval.

Colour maps are produced by interpolating the grid down to the pixel size. The parameter is then incremented with respect to specific amplitude ranges to provide colour "contour" maps.

Monochromatic shadow maps or images are generated by employing an artificial sun to cast shadows on a surface defined by the geophysical grid. There are many variations in the shadowing technique. These techniques can be applied to total field or enhanced magnetic data, magnetic derivatives, resistivity, etc. The shadowing technique is also used as a quality control method to detect subtle changes between lines.

Multi-channel Stacked Profiles

Distance-based profiles of the digitally recorded geophysical data are generated and plotted at an appropriate scale. These profiles also contain the calculated parameters that are used in the interpretation process. These are produced as worksheets prior to interpretation, and are also presented in the final corrected form after interpretation. The profiles display electromagnetic anomalies with their respective interpretive symbols. Table 5-1 shows the parameters and scales for the multi-channel stacked profiles.

In Table 5-1, the log resistivity scale of 0.06 decade/mm means that the resistivity changes by an order of magnitude in 16.6 mm. The resistivities at 0, 33 and 67 mm up from the bottom of the digital profile are respectively 1, 100 and 10,000 ohm-m.

Table 5-1. Multi-channel Stacked Profiles

Channel Name (Freq)	Observed Parameters	Scale Units/mm
MAG20	total magnetic field (fine)	20 nT
MAG200	total magnetic field (coarse)	200 nT
ALTBIRDM	EM sensor height above ground	6 m
CXI1000	vertical coaxial coil-pair in-phase (1000 Hz)	2 ppm
CXQ1000	vertical coaxial coil-pair quadrature (1000 Hz)	2 ppm
CPI900	horizontal coplanar coil-pair in-phase (900 Hz)	4 ppm
CPQ900	horizontal coplanar coil-pair quadrature (900 Hz)	4 ppm
CXI5500	vertical coaxial coil-pair in-phase (5500 Hz)	4 ppm
CXQ5500	vertical coaxial coil-pair quadrature (5500 Hz)	4 ppm
CPI7200	horizontal coplanar coil-pair in-phase (7200 Hz)	10 ppm
CPQ7200	horizontal coplanar coil-pair quadrature (7200 Hz)	10 ppm
CPI56K	horizontal coplanar coil-pair in-phase (56,000 Hz)	20 ppm
CPQ56K	horizontal coplanar coil-pair quadrature (56,000 Hz)	20 ppm
	Computed Parameters	
DIFI (mid freq.)	difference function in-phase from CXI and CPI	4 ppm
DIFQ (mid freq.)	difference function quadrature from CXQ and CPQ	4 ppm
RES900	log resistivity	.06 decade
RES7200	log resistivity	.06 decade
RES56K	log resistivity	.06 decade
DEP900	apparent depth	6 m
DEP7200	apparent depth	6 m
DEP56K	apparent depth	6 m
CDT	conductance	1 grade

6. PRODUCTS

This section lists the final maps and products that have been provided under the terms of the survey agreement. Other products can be prepared from the existing dataset, if requested. These include magnetic enhancements or derivatives, percent magnetite, resistivities corrected for magnetic permeability and/or dielectric permittivity, digital terrain, resistivity-depth sections, inversions, overburden thickness, and radiometric ratios. Most parameters can be displayed as contours, profiles, or in colour.

Base Maps

Base maps of the survey area were produced from digital topography (BCTRIM data) supplied by Strongbow Exploration Inc. This process provides a relatively accurate, distortion-free base that facilitates correlation of the navigation data to the map coordinate system. The topographic files were combined with geophysical data for plotting the final maps. All maps were created using the following parameters:

Projection Description:

Datum:	NAD83		
Ellipsoid:	GRS 1980		
Projection:	UTM (Zone: 10N)		
Central Meridian:	123°		
False Northing:	0		
False Easting:	500000		
Scale Factor:	0.9996		
WGS84 to Local Conversion:	Molodensky		
Datum Shifts:	DX: 0	DY: 0	DZ: 0

The following parameters are presented on single map sheets, at scales of 1:10,000 and 1:7,500. All maps include flight lines and topography, unless otherwise indicated. Preliminary products are not listed.

Final Products

	No. of Map Sets		
	Mylar	Blackline	Colour
EM Anomalies		2	
Total Magnetic Field			2
Calculated Vertical Magnetic Gradient			2
Apparent Resistivity 7200 Hz			2
Apparent Resistivity 56,000 Hz			2

Additional Products

Digital Archive (see Archive Description)	1 CD-ROM
Survey Report	2 copies
Multi-channel Stacked Profiles	All lines
Flight Path Video (VHS)	1 cassette

7. SURVEY RESULTS

General Discussion

Table 7-1 summarizes the EM responses in the survey area, with respect to conductance grade and interpretation. The apparent conductance and depth values shown in the EM Anomaly list appended to this report have been calculated from "local" in-phase and quadrature amplitudes of the Coaxial 5500 Hz frequency. The picking and interpretation procedure relies on several parameters and calculated functions. For this survey, the Coaxial 5500 Hz responses and the mid-frequency difference channels were used as two of the main picking criteria. The 7200 Hz coplanar results were also weighted to provide picks over wider or flat-dipping sources. The quadrature channels provided picks in areas where the in-phase responses might have been suppressed by magnetite.

The anomalies shown on the electromagnetic anomaly maps are based on a near-vertical, half plane model. This model best reflects "discrete" bedrock conductors. Wide bedrock conductors or flat-lying conductive units, whether from surficial or bedrock sources, may give rise to very broad anomalous responses on the EM profiles. These may not appear on the electromagnetic anomaly map if they have a regional character rather than a locally anomalous character.

TABLE 7-1 EM ANOMALY STATISTICS

SKOONKA CREEK AREA, B.C.

CONDUCTOR GRADE	CONDUCTANCE RANGE SIEMENS (MHOS)	NUMBER OF RESPONSES
7	>100	0
6	50 - 100	0
5	20 - 50	0
4	10 - 20	1
3	5 - 10	2
2	1 - 5	94
1	<1	239
*	INDETERMINATE	148
TOTAL		484

CONDUCTOR MODEL	MOST LIKELY SOURCE	NUMBER OF RESPONSES
D	THIN BEDROCK CONDUCTOR	4
B	DISCRETE BEDROCK CONDUCTOR	25
S	CONDUCTIVE COVER	412
H	ROCK UNIT OR THICK COVER	6
E	EDGE OF WIDE CONDUCTOR	37
TOTAL		484

(SEE EM MAP LEGEND FOR EXPLANATIONS)

These broad conductors, which more closely approximate a half-space model, will be maximum coupled to the horizontal (coplanar) coil-pair and should be more evident on the resistivity parameter. Resistivity maps, therefore, may be more valuable than the electromagnetic anomaly maps, in areas where broad or flat-lying conductors are considered to be of importance. Contoured resistivity maps, based on the 7200 Hz and 56kHz coplanar data are included with this report.

Excellent resolution and discrimination of conductors was accomplished by using a fast sampling rate of 0.1 sec and by employing a "common" frequency (5500/7200 Hz) on two orthogonal coil-pairs (coaxial and coplanar). The resulting difference channel parameters often permit differentiation of bedrock and surficial conductors, even though they may exhibit similar conductance values.

Anomalies that occur near the ends of the survey lines (i.e., outside the survey area), should be viewed with caution. Some of the weaker anomalies could be due to aerodynamic noise, i.e., bird bending, which is created by abnormal stresses to which the bird is subjected during the climb and turn of the aircraft between lines. Such aerodynamic noise is usually manifested by an anomaly on the coaxial in-phase channel only, although severe stresses can affect the coplanar in-phase channels as well.

Magnetics

A Fugro CF-1 cesium vapour magnetometer was operated at the survey base to record diurnal variations of the earth's magnetic field. The clock of the base station was synchronized with that of the airborne system to permit subsequent removal of diurnal drift. A GEM Systems GSM-19T proton precession magnetometer was also operated as a backup unit.

The total magnetic field data have been presented as contours on the base maps using a contour interval of 10 nT where gradients permit. The map shows the magnetic properties of the rock units underlying the survey area.

The total magnetic field data have been subjected to a processing algorithm to produce maps of the calculated vertical gradient. This procedure enhances near-surface magnetic units and suppresses regional gradients. It also provides better definition and resolution of magnetic units and displays weak magnetic features that may not be clearly evident on the total field maps.

There is some evidence on the magnetic maps that suggests that the survey area has been subjected to deformation and/or alteration. These structural complexities are evident on the contour maps as variations in magnetic intensity, irregular patterns, and as offsets or changes in strike direction.

If a specific magnetic intensity can be assigned to the rock type that is believed to host the target mineralization, it may be possible to select areas of higher priority on the basis of the total field magnetic data. This is based on the assumption that the magnetite content of the host rocks will give rise to a limited range of contour values that will permit differentiation of various lithological units.

The magnetic results, in conjunction with the other geophysical parameters, have provided valuable information that can be used to help map the geology and structure in the survey area.

Apparent Resistivity

Apparent resistivity maps, which display the conductive properties of the survey area, were produced from the 7200 Hz and 56,000 Hz coplanar data. The maximum resistivity values, which are calculated for each frequency, are 8,400 and 25,000 ohm-m respectively. These cutoffs eliminate the erratic higher resistivities that would result from unstable ratios of very small EM amplitudes.

In general, the resistivity patterns show only moderate agreement with the magnetic trends. This suggests that many of the resistivity lows are probably related to conductive overburden or alluvial material in the valleys, rather than bedrock conductors. There are some areas where resistivity highs correlate with magnetic highs (due to increases in magnetite) and other areas where resistivity highs correlate with magnetic lows (due to non-magnetic siliceous units). Most of the resistivity lows appear to be associated with topographic lows, although there are at least four obvious exceptions.

The low-sulphide, banded quartz veins that host the auriferous mineralization would not be expected to yield a conductive or magnetic response. The targets are more likely to yield resistivities that are higher than background, associated with relative magnetic lows. The EM anomalies are considered to be of little value, except in areas that exhibit an increase in alteration, porosity (shear zones) or sulphide content. The magnetic lows should be better suited to mapping the quartz-rich units and silicic alteration if they exhibit sufficient width and are not obscured by variations in the more magnetic volcanic flows.

Electromagnetic Anomalies

The EM anomalies resulting from this survey appear to fall within one of these general categories. The first type consists of discrete, well-defined anomalies that yield marked inflections on the difference channels. These anomalies are usually attributed to conductive sulphides or graphite and are generally given a "B", "T" or "D" interpretive symbol, denoting a bedrock source. There were very few anomalies of this type detected in the survey area.

The second class of anomalies comprises moderately broad responses that exhibit the characteristics of a half-space and do not yield well-defined inflections on the difference channels. Anomalies in this category are usually given an "S" or "H" interpretive symbol. The lack of a difference channel response usually implies a broad or flat-lying conductive source such as overburden. Some of these anomalies could reflect conductive rock units, zones of deep weathering, or altered intrusives, all of which can yield “non-discrete” signatures.

The effects of conductive overburden are evident over portions of the survey area. Although the difference channels (DIFI and DIFQ) are extremely valuable in detecting bedrock conductors that are partially masked by conductive overburden, sharp undulations in the bedrock/overburden interface can yield anomalies in the difference channels which may be interpreted as possible bedrock conductors. Such anomalies usually fall into the "S?" or "B?" classification but may also be given an "E" interpretive symbol, denoting a resistivity contrast at the edge of a conductive unit.

The "?" symbol does not question the validity of an anomaly, but instead indicates some degree of uncertainty as to which is the most appropriate EM source model. This ambiguity results from the combination of effects from two or more sources, such as overburden and bedrock, gradational changes, moderately shallow dips, or the presence of magnetite. The presence of a conductive upper layer has a tendency to mask or alter the characteristics of bedrock conductors, making interpretation difficult. This problem is further exacerbated in the presence of magnetite.

The third anomaly category includes responses that are associated with magnetite. Magnetite can cause suppression or polarity reversals of the in-phase components, particularly at the lower frequencies in resistive areas. The effects of magnetite-rich rock units are usually evident on the multi-parameter geophysical data profiles as negative excursions of the lower frequency in-phase channels. Skarn deposits often yield signatures of this type.

In areas where EM responses are evident primarily on the quadrature components, zones of poor conductivity are indicated. Where these responses are coincident with magnetic anomalies, it is possible that the in-phase component amplitudes have been suppressed by the effects of magnetite. Poorly-conductive magnetic features can give rise to resistivity anomalies that are only slightly below or slightly above background. As it is expected that poorly-conductive economic mineralization could be associated with magnetite-rich units, many of these weakly anomalous features are considered to be of interest. In areas where magnetite causes the in-phase components to become negative, the apparent conductance and depth of EM anomalies will be unreliable. Magnetite effects usually give rise to overstated (higher) resistivity values and understated (shallow) depth calculations.

As potential targets within the area may be associated with extremely low-sulphide, quartz-rich units that are non-magnetic, it is impractical to assess the relative merits of EM anomalies on the basis of conductance. It is recommended that an attempt be made to compile a suite of geophysical "signatures" over any known areas of interest. Anomaly characteristics are clearly defined on the multi-parameter geophysical data profiles that are supplied as one of the survey products.

Potential Targets in the Survey Area

The electromagnetic anomaly map shows the anomaly locations with the interpreted conductor type, dip, conductance and depth being indicated by symbols. Direct magnetic correlation is also shown if it exists. No conductor axes have been shown on the EM anomaly maps, because very few bedrock anomalies could be correlated from line to line with a reasonable degree of confidence.

JJ

The JJ Zone outcrops in the vicinity of fiducial 4449 on line 10110 (UTM 606050E,5578600N). The mineralized zone reportedly strikes about 070° and dips to the southeast. The banded quartz veins are up to 4 m wide and the auriferous material has a strike length of more than 350 m.

The airborne profiles over the zone on line 10110 do not yield a distinctive, clearly-defined geophysical response, although the CP900 inphase shows a subtle dip over the zone that is associated with a moderately weak magnetic trough. Anomaly 10110C, about 50 m to the south, marks the southern edge of a broad (200 m wide) moderately conductive zone that also hosts anomaly 10110D. The latter has been attributed to probable surficial cover that follows the southwest-trending topographic low.

Anomaly 10100D suggests a possible bedrock conductor to the southwest that is on strike with JJ. This conductor also correlates with the same magnetic low. Anomalies 10090D and 10080E are also on strike, along the same magnetic low. These have been attributed to edge effects (resistivity contrasts at the south edge of the conductive zone) but could be due in part to alteration associated with the banded quartz veins. The EM signature may be too ambiguous to be used as an effective criterion for locating similarly mineralized zones, but the fairly prominent vertical gradient magnetic low continues southwest beyond the property boundary. The magnetic parameter appears to be a more effective tool in this area for defining the quartz-rich host unit.

Discovery

The Discovery Zone outcrops in the vicinity of fiducial 9677 on line 10252 (UTM 5581185N,607450E). Anomaly 10252C is coincident with this zone. It is interesting to note that this anomaly is located near the northern contact of a strong magnetic high, and yields a magnetic correlation of 1473 nT. The negative inphase response suggests a magnetite content of about 5.0%. The subtle quadrature responses suggest a broad source that is associated with, or overlies, the magnetite-rich unit. If the Discovery Zone is also associated with a non-magnetic silicified intrusive, its magnetic (low) response has been completely obscured by the strong magnetic high to the south. However, the vertical gradient map does suggest the presence of a northeast to east-northeast trending magnetic low at the northern contact.

The Discovery Zone occurs within a large ovate resistivity high that extends northeast from 10240H to the intersection of line 10300 and tie line 19010. Most of this apparent resistivity high is due to the effects of magnetite, particularly near 10250C in the southwestern portion.

The magnetic anomaly is probably due to volcanic flows. The fact that the inferred northern contact of this unit, and the central axis of the resistivity low, both parallel the elevation contours on a northwest-facing slope, suggests that the flows could be flat-lying and that they may have been eroded or incised. It is interesting to note that most of the non-magnetic units in the area appear to be associated with topographic lows. This tends to support the hypothesis that the lower elevation (non-magnetic) units are partially overlain by the more magnetic flows.

Although the known mineralization is associated with 070°-trending banded quartz zones that appear to be non-magnetic and non-conductive, the following table lists a few anomalous zones that could reflect increases in conductivity (shears or alteration zones) that may be of bedrock origin. Given the physical properties of the known mineralized zones, some of these very weak responses could be of interest, particularly if they are associated with magnetic lows.

Anomaly	Type	Mag	Comments
10010G 10010I 10010J	B? B? B?	- 653 47	Anomaly 10010G occurs on the southern edge of a magnetic low, while 10010I and 10010J are both coincident with magnetic highs. Anomaly 10010G is located in a creek bed, and is likely influenced by conductive alluvium. The small coplanar trough on the 7200 Hz profile at 10010J is likely due to magnetite, rather than a resistive intrusive. It is on high ground and should be open to the west.
10020J 10020O	B B	- -	Anomaly 10020J is on a hill, and indicates a short, thin source on a magnetic contact. Anomaly 10020O is located in a creek that yields a moderate resistivity low. This thin source is at the northern edge of an interesting, plug-like magnetic low that tends to enhance its significance.
10030C	D	248	This anomaly is part of one of the more clearly defined bedrock conductors on the property. The thin source at 10030C yields a 248 nT magnetic correlation, but the profiles and the vertical gradient data show that it actually coincides with a subtle magnetic low on the south flank of a stronger magnetic unit. Anomalies 10050B and 10060C, to the ENE, clearly follow this contact. Anomaly 10090C may be part of the same NE-trending, 500 m-long conductor, but it is much weaker and associated with a local magnetic high. The most conductive portion is near 10020B, while the anomalies east of 10060C are in a magnetite-induced resistivity high. Anomaly 10030C is considered to be the most attractive target, where a thin, north-dipping source is indicated. Anomalies 10040B and 10050B, however, suggest possible dips to the south.
10030F	B?	88	This short, thin conductor gives rise to an 88 nT coincident magnetic response, but it is located near the northern contact of a small, well-defined, NE-trending magnetic low. It occurs near the northern edge of a prominent resistivity low that strikes 052° along SW and NE-trending creeks, separated by a (conductive) ridge at 10070P.
10040J	S?	382	This high amplitude response has been attributed to a possible surficial source. However, the apparent shallow depth might be due to magnetite. As with some of the previous anomalies, it yields an apparent magnetic correlation, but actually

Anomaly	Type	Mag	Comments
			correlates with a very subtle magnetic dip on the south flank of a local magnetic high. The oblate resistivity low occurs near a road junction, on relatively high ground, and could reflect an alteration plug.
10060K	B?	68	This thin source also yields an apparent magnetic coincidence, but actually correlates with a small 68 nT magnetic low within a larger high. It is located on high ground, near the northern edge of a moderate, oblate resistivity low. The prominent resistivity high to the north is due to magnetite suppression.
10070E 10100D	S? B	- -	Anomaly 10070E is probably surficial, but it occurs on a ridge, and gives rise to a strong resistivity low that correlates with an ENE-trending magnetic low that is on strike with the JJ Zone. The conductor becomes broader and less distinct towards the WSW, but the magnetic low persists through 10050C. Anomaly 10110D is at the south edge of a broad resistivity low, but on the same magnetic low that hosts the JJ Zone. This thin conductor is probably due to alteration associated with the mineralized quartz-rich unit. The JJ Zone outcrops on the adjacent line, between 10110C and 10110D. Anomaly 10110C is on the northwestern flank of a small magnetic high.
10090A	D	226	A short, thin conductor of very limited strike extent is also observed on tie line 19050. This conductor also appears to be associated with a magnetic contact.
10100I	B?	491	This interesting response reflects a thin source located on a ridge between two creeks. The ridge is magnetic, and because of magnetite suppression, there is no distinct resistivity low.
10120B	S?	-	This weak response is of interest because it is associated with a 060° trending magnetic low, similar to that which hosts the JJ Zone. However, the magnetic low at 10120B correlates with negative inphase responses due to magnetite. The magnetic low has therefore been attributed to remanent magnetization on this line.
10120J	E	726	Although this response yields an apparent coincident magnetic correlation, it actually occurs in a strong, sharp, SE-trending magnetic low that is likely due to remanent magnetization. (The inphase

Anomaly	Type	Mag	Comments
			low correlates with the magnetic low.)
10140B	S?	1438	A strong magnetic anomaly hosts 10140B. The quadrature anomalies suggest that this magnetite-rich zone is weakly conductive.
10160D 10160E	S? B?	- 313	Anomaly 10160D correlates with a 058° magnetic low that is sub-parallel to the JJ Zone. Like 10120B and 10120J, the magnetic low correlates with negative inphase (reversed magnetization). Anomaly 10160E, about 150 m to the north, occurs on the southern contact of a local magnetic high. This thin, very weak conductor is on strike with the JJ Zone, and could be related to the same structure.
10180G 10180H	S? E	- 1324	A small circular magnetic high occurs just north of a bend in a south-flanking linear magnetic low, where the strike changes from 067° to 045°, close to the intersection with a third inferred (SE) break through 10200G. A high soil anomaly occurs near the eastern margin of this interesting plug-like magnetic feature. Increased quadrature responses suggest that this magnetite-rich unit is weakly conductive. Anomaly 10180G indicates a thin conductor within the broader zone, that correlates with the northern contact of a strong magnetic low. Anomaly 10180H occurs on the northeastern perimeter of the magnetic unit, while 10190E is near its southeastern contact. The proximal soil anomaly and the inferred structure both tend to enhance the significance of these responses, particularly near 10180G.
10190C	S	-	Anomaly 10190C has been attributed to near-surface conductivity, but the coaxial responses suggest the presence of a weakly conductive thin source. The flanking anomalies 10190B and 10190D, both of which occur on magnetic gradients, could also reflect bedrock sources. Anomaly 10190C is of interest because of a coincident soil high and its location within a prominent, broad magnetic low.
10220F 10220G	E S	- -	These two anomalies occur within a creek valley. Although both could be due to conductive alluvium, they are associated with a moderately strong magnetic low at the junction of 055° and 135° inferred linear trends. The magnetic low correlates with negative inphase responses, which might reflect reversed magnetization. Anomaly 10220H

Anomaly	Type	Mag	Comments
			yields a moderate resistivity low at the centre of the property. It follows creek bed and is probably due to near surface conductivity. However, it is associated with the south contact of a NE-trending magnetic low, near its intersection with the SSE-trending linear low. Its location, about 150 m east of a soil high tends to further enhance its significance.
10252C	S?	1473	This anomaly is over the Discovery Zone. The moderately broad quadrature responses are associated with negative inphase responses that are caused by the moderately strong elongate ENE-trending magnetic unit. As the Discovery Zone is reportedly hosted by the same (non-magnetic, quartz-rich) rock type that hosts the JJ deposit, it appears that anomaly 10252C is coincidental, and that the system is not seeing the auriferous quartz veins. Any associated magnetic low has been obscured by the prominent magnetic high. The only geophysical signature that is common to both the JJ and Discovery zones is that the vertical gradient map suggests they are both associated with magnetic contacts that strike roughly 060°. The Discovery zone is located within a broad NE-trending resistivity high that is at least partially due to magnetite suppression. It is probably coincidental that the local soil anomaly correlates with the magnetic high.
10270E	B	-	Anomaly 10270E reflects a thin, moderately weak conductor that is located less than 100 m up-stream from the Gold Creek soil anomaly. The conductor is associated with a local magnetic low that occurs at the possible intersection of 060° and 120° trending linear features. This is considered to be a moderately attractive target.
10280G	S	-	A broad, weak, near-surface resistivity low straddles a creek bed that is associated with a WNW-trending magnetic low. This resistivity low/magnetic low is coincident with the Ember soil high.
10300A	S?	-	The magnetite content of a moderate, east-trending magnetic anomaly gives rise to a resistivity high. The associated quadrature responses, such as 10300A, suggest that the magnetic unit is weakly conductive.
10310E	B?	-	A subtle conductor of probable bedrock origin is

Anomaly	Type	Mag	Comments
			associated with an ENE-trending magnetic low. This interesting response is less than 100 m south of a soil anomaly, and is therefore considered to be a target that warrants further investigation. Although the conductor appears to be of very limited strike length, the associated magnetic low strikes roughly 058° over a distance of at least 1.5 km.
10341B	B?	-	A subtle resistivity low correlates with an east-trending (077°) creek, east of line 10310, and east of a well-defined SE-trending contact near 10310B. Anomaly 10341B is hosted by the broad non-magnetic unit east of the contact. The shape of the non-magnetic unit correlates closely with the weak resistivity low. The discrete anomaly at 10341B has been attributed to a thin bedrock source, but it is located near the confluence of two creeks. High soil values have been observed about 500 m downstream, on line 10390.
10350F	B?	-	This poorly-defined response is hosted by a weak, SE-trending magnetic low.
10360F	S?	-	This extremely weak, poorly defined anomaly is not an attractive geophysical response, but it is in close proximity to the Backburn soil anomaly. It is located near the southwestern flank of an ovate magnetic high in a relatively resistive unit.
10360A 10380A	S S	- 51	These anomalies are within the same non-magnetic, weakly conductive unit that hosts anomaly 10341B. Anomaly 10360A may be due to a moderately broad, buried unit that gives rise to a moderately strong resistivity low. The conductor is associated with a small creek, but only in this area. Anomaly 10380A is extremely weak, but correlates with the edge of a weak magnetic high. Its significance is enhanced by its proximity to a soil high. A second soil anomaly is evident in the creek bed about 250 m to the NNE, just west of anomaly 10400B.
10390D	S	11	Anomaly 10390D may be a reflection of a slightly lower flying height. However, this anomaly is located in a creek, on a SE-trending magnetic contact, in a very weak resistivity low. It is situated near the southern limit of the Backburn soil anomaly.
10430B	B?	-	This very weak response is within the system noise

Anomaly	Type	Mag	Comments
			envelope, and could be due to spheric spikes, rather than a bedrock source. This response is associated with a north-trending creek, and is considered to be of extremely low priority, unless it occurs in an area of favourable geology.

8. CONCLUSIONS AND RECOMMENDATIONS

This report provides a very brief description of the survey results and describes the equipment, data processing procedures and logistics of the survey.

Neither the JJ nor the Discovery showings yielded clearly defined EM signatures that could be used to locate other similarly mineralized zones on the property. However, it is believed that the linear magnetic lows that follow the favourable 060°-070° alignment direction could reflect the favourable quartz-rich hosts. Both the JJ and Discovery showings are in close proximity to magnetic contacts.

There are no anomalies in the survey block that are typical of massive sulphide responses. However, the survey was successful in locating a few weak or broad responses that may warrant additional work. The various maps included with this report display the magnetic and conductive properties of the survey area. It is recommended that a complete assessment and detailed evaluation of the survey results be carried out, in conjunction with all available geophysical, geological and geochemical information. Particular reference should be made to the multi-parameter data profiles that clearly define the characteristics of the individual anomalies.

Most anomalies in the area are moderately weak and poorly-defined. Many have been attributed to conductive overburden or deep weathering, although several are associated with magnetite-rich rock units. Some of these yield responses stronger than those observed over the known showings. Others coincide with magnetic gradients that may reflect contacts, faults, shears or alteration zones. Such structural breaks are considered to be of particular interest as they may have influenced mineral deposition within the survey area.

The interpreted conductors, resistive units and magnetic lows defined by the survey should be subjected to further investigation, using appropriate surface exploration techniques. Anomalies that are currently considered to be of moderately low priority may require upgrading if follow-up results are favourable. In the search for quartz-hosted auriferous mineralization, some of the linear resistivity highs could also prove to be potential target areas.

It is also recommended that image processing of existing geophysical data be considered, in order to extract the maximum amount of information from the survey results. Current software and imaging techniques often provide valuable information on structure and lithology, which may not be clearly evident on the contour and colour maps. These techniques can yield images that define subtle, but significant, structural details.

Respectfully submitted,

FUGRO AIRBORNE SURVEYS CORP.

Paul A. Smith
Geophysicist

R06004MAR.06

APPENDIX A

LIST OF PERSONNEL

The following personnel were involved in the acquisition, processing, interpretation and presentation of data, relating to a DIGHEM airborne geophysical survey carried out for Strongbow Exploration Inc., over the Skoonka Creek Property, B.C.

David Miles	Manager, Helicopter Operations
Emily Farquhar	Manager, Data Processing and Interpretation
Delvin Masilamani	Senior Geophysical Operator
Amanda Heydorn	Field Geophysicist/Crew Leader
Guy Lajoie	Pilot (Questral Helicopters Ltd.)
Elizabeth Bowslaugh	Geophysicist/Data Processor
Paul A. Smith	Interpretation Geophysicist
Lyn Vanderstarren	Drafting Supervisor
Susan Pothiah	Word Processing Operator
Albina Tonello	Secretary/Expeditor

The survey consisted of 207 km of coverage, flown from January 23 to January 25, 2006.

All personnel are employees of Fugro Airborne Surveys, except for the pilot who is an employee of Questral Helicopters Ltd.

APPENDIX B

DATA PROCESSING FLOWCHARTS

APPENDIX B

Processing Flow Chart - Electromagnetic Data

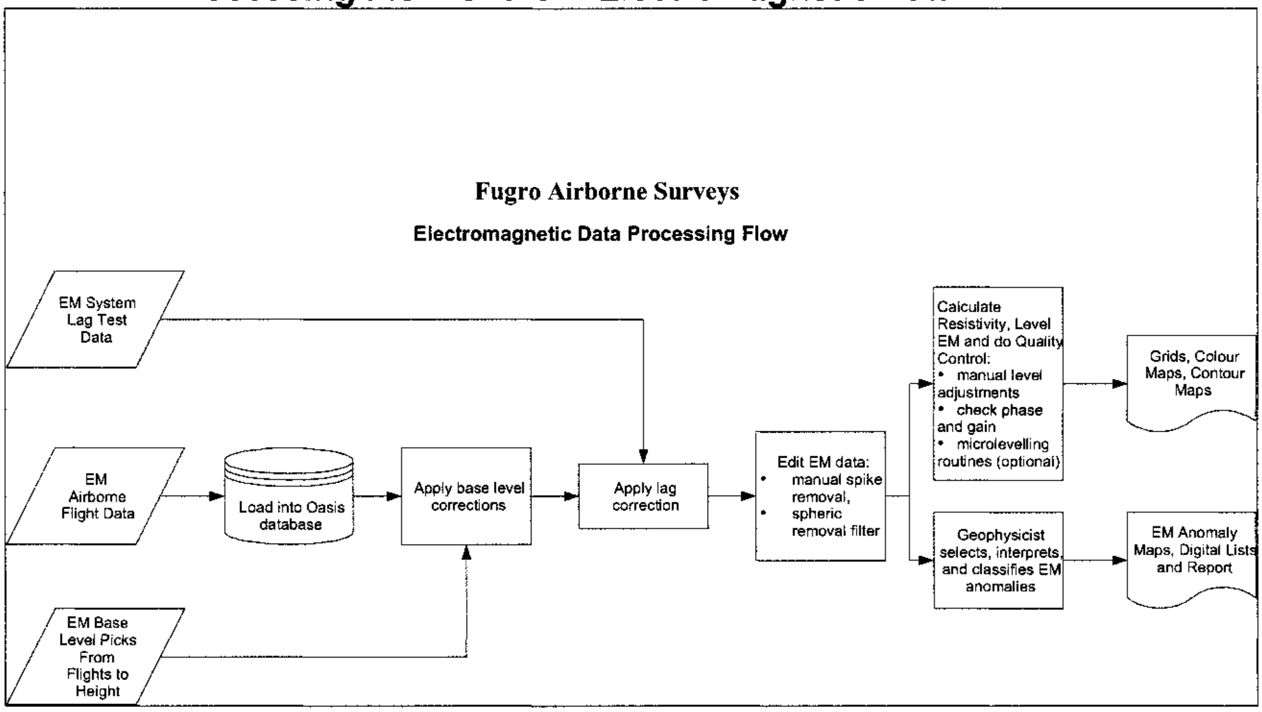

Processing Flow Chart - Magnetic Data

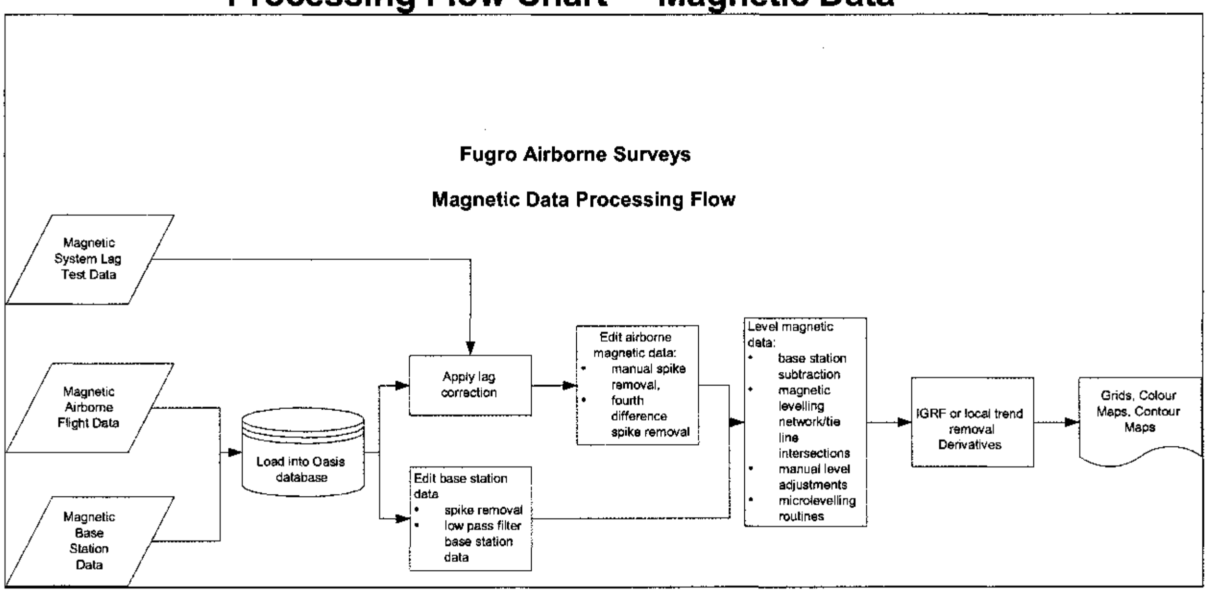

APPENDIX C

BACKGROUND INFORMATION

BACKGROUND INFORMATION

Electromagnetics

Fugro electromagnetic responses fall into two general classes, discrete and broad. The discrete class consists of sharp, well-defined anomalies from discrete conductors such as sulphide lenses and steeply dipping sheets of graphite and sulphides. The broad class consists of wide anomalies from conductors having a large horizontal surface such as flatly dipping graphite or sulphide sheets, saline water-saturated sedimentary formations, conductive overburden and rock, kimberlite pipes and geothermal zones. A vertical conductive slab with a width of 200 m would straddle these two classes.

The vertical sheet (half plane) is the most common model used for the analysis of discrete conductors. All anomalies plotted on the geophysical maps are analyzed according to this model. The following section entitled **Discrete Conductor Analysis** describes this model in detail, including the effect of using it on anomalies caused by broad conductors such as conductive overburden.

The conductive earth (half-space) model is suitable for broad conductors. Resistivity contour maps result from the use of this model. A later section entitled **Resistivity Mapping** describes the method further, including the effect of using it on anomalies caused by discrete conductors such as sulphide bodies.

Geometric Interpretation

The geophysical interpreter attempts to determine the geometric shape and dip of the conductor. Figure C-1 shows typical HEM anomaly shapes which are used to guide the geometric interpretation.

Discrete Conductor Analysis

The EM anomalies appearing on the electromagnetic map are analyzed by computer to give the conductance (i.e., conductivity-thickness product) in siemens (mhos) of a vertical sheet model. This is done regardless of the interpreted geometric shape of the conductor. This is not an unreasonable procedure, because the computed conductance increases as the electrical quality of the conductor increases, regardless of its true shape. DIGHEM anomalies are divided into seven grades of conductance, as shown in Table C-1. The conductance in siemens (mhos) is the reciprocal of resistance in ohms.

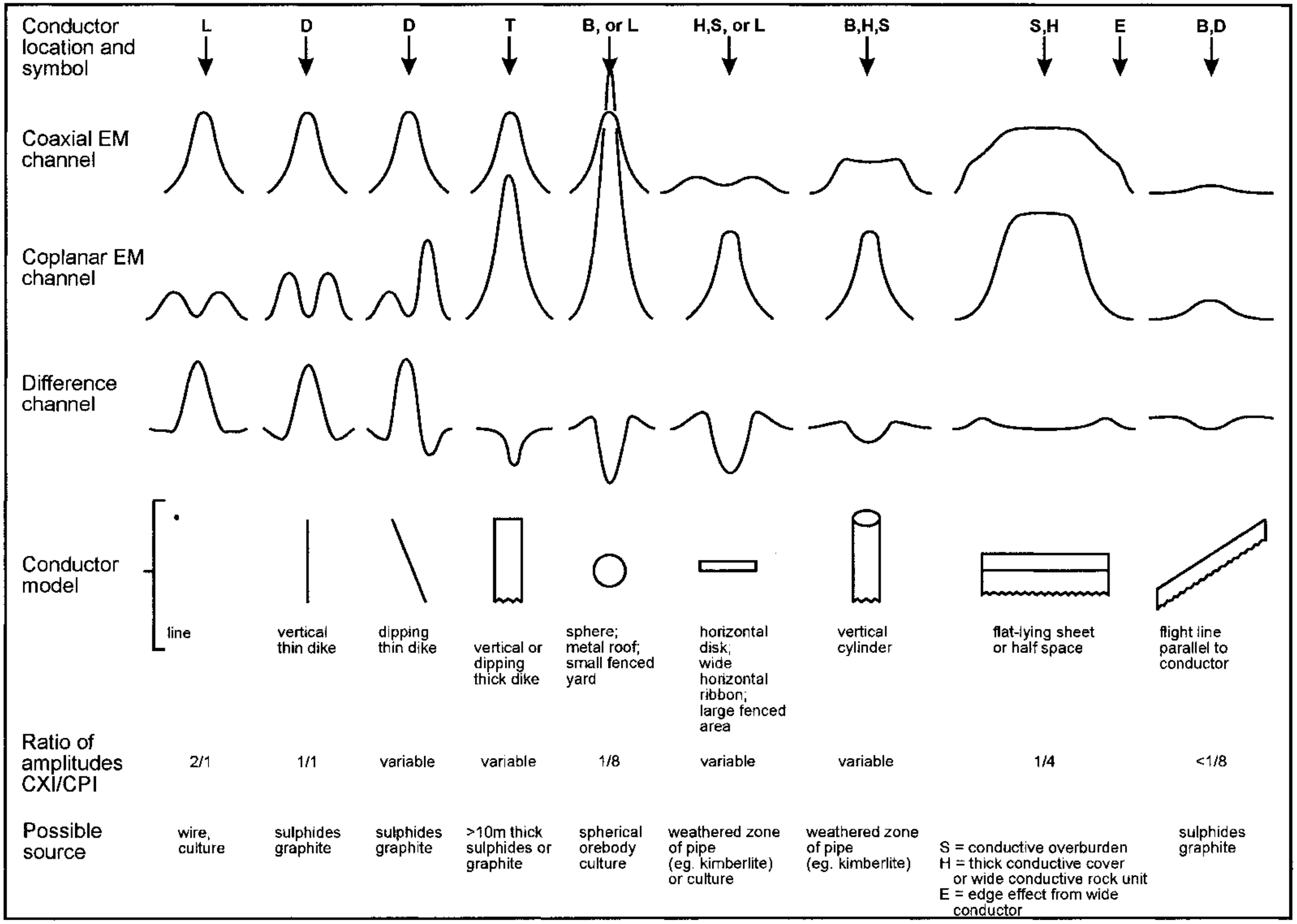

Typical HEM anomaly shapes

Figure C-1

The conductance value is a geological parameter because it is a characteristic of the conductor alone. It generally is independent of frequency, flying height or depth of burial, apart from the averaging over a greater portion of the conductor as height increases. Small anomalies from deeply buried strong conductors are not confused with small anomalies from shallow weak conductors because the former will have larger conductance values.

Table C-1. EM Anomaly Grades

Anomaly Grade	Siemens
7	> 100
6	50 - 100
5	20 - 50
4	10 - 20
3	5 - 10
2	1 - 5
1	< 1

Conductive overburden generally produces broad EM responses which may not be shown as anomalies on the geophysical maps. However, patchy conductive overburden in otherwise resistive areas can yield discrete anomalies with a conductance grade (cf. Table C-1) of 1, 2 or even 3 for conducting clays which have resistivities as low as 50 ohm-m. In areas where ground resistivities are below 10 ohm-m, anomalies caused by weathering variations and similar causes can have any conductance grade. The anomaly shapes from the multiple coils often allow such conductors to be recognized, and these are indicated by the letters S, H, and sometimes E on the geophysical maps (see EM legend on maps).

For bedrock conductors, the higher anomaly grades indicate increasingly higher conductances. Examples: the New Insco copper discovery (Noranda, Canada) yielded a grade 5 anomaly, as did the neighbouring copper-zinc Magusi River ore body; Mattabi (copper-zinc, Sturgeon Lake, Canada) and Whistle (nickel, Sudbury, Canada) gave grade 6; and the Montcalm nickel-copper discovery (Timmins, Canada) yielded a grade 7 anomaly. Graphite and sulphides can span all grades but, in any particular survey area, field work may show that the different grades indicate different types of conductors.

Strong conductors (i.e., grades 6 and 7) are characteristic of massive sulphides or graphite. Moderate conductors (grades 4 and 5) typically reflect graphite or sulphides of a less massive character, while weak bedrock conductors (grades 1 to 3) can signify poorly connected graphite or heavily disseminated sulphides. Grades 1 and 2 conductors may not respond to ground EM equipment using frequencies less than 2000 Hz.

The presence of sphalerite or gangue can result in ore deposits having weak to moderate conductances. As an example, the three million ton lead-zinc deposit of Restigouche Mining Corporation near Bathurst, Canada, yielded a well-defined grade 2 conductor. The 10 percent by volume of sphalerite occurs as a coating around the fine grained massive pyrite, thereby inhibiting electrical conduction. Faults, fractures and shear zones may produce anomalies that typically have low conductances (e.g., grades 1 to 3). Conductive rock formations can yield anomalies of any conductance grade. The conductive materials in such rock formations can be salt water, weathered products such as clays, original depositional clays, and carbonaceous material.

For each interpreted electromagnetic anomaly on the geophysical maps, a letter identifier and an interpretive symbol are plotted beside the EM grade symbol. The horizontal rows of dots, under the interpretive symbol, indicate the anomaly amplitude on the flight record. The vertical column of dots, under the anomaly letter, gives the estimated depth. In areas where anomalies are crowded, the letter identifiers, interpretive symbols and dots may be obliterated. The EM grade symbols, however, will always be discernible, and the obliterated information can be obtained from the anomaly listing appended to this report.

The purpose of indicating the anomaly amplitude by dots is to provide an estimate of the reliability of the conductance calculation. Thus, a conductance value obtained from a large ppm anomaly (3 or 4 dots) will tend to be accurate whereas one obtained from a small ppm anomaly (no dots) could be quite inaccurate. The absence of amplitude dots indicates that the anomaly from the coaxial coil-pair is 5 ppm or less on both the in-phase and quadrature channels. Such small anomalies could reflect a weak conductor at the surface or a stronger conductor at depth. The conductance grade and depth estimate illustrates which of these possibilities fits the recorded data best.

The conductance measurement is considered more reliable than the depth estimate. There are a number of factors that can produce an error in the depth estimate, including the averaging of topographic variations by the altimeter, overlying conductive overburden, and the location and attitude of the conductor relative to the flight line. Conductor location and attitude can provide an erroneous depth estimate because the stronger part of the conductor may be deeper or to one side of the flight line, or because it has a shallow dip. A heavy tree cover can also produce errors in depth estimates. This is because the depth estimate is computed as the distance of bird from conductor, minus the altimeter reading. The altimeter can lock onto the top of a dense forest canopy. This situation yields an erroneously large depth estimate but does not affect the conductance estimate.

Dip symbols are used to indicate the direction of dip of conductors. These symbols are used only when the anomaly shapes are unambiguous, which usually requires a fairly resistive environment.

A further interpretation is presented on the EM map by means of the line-to-line correlation of bedrock anomalies, which is based on a comparison of anomaly shapes on adjacent lines. This provides conductor axes that may define the geological structure over portions of the survey area. The absence of conductor axes in an area implies that anomalies could not be correlated from line to line with reasonable confidence.

The electromagnetic anomalies are designed to provide a correct impression of conductor quality by means of the conductance grade symbols. The symbols can stand alone with geology when planning a follow-up program. The actual conductance values are printed in the attached anomaly list for those who wish quantitative data. The anomaly ppm and depth are indicated by inconspicuous dots which should not distract from the conductor patterns, while being helpful to those who wish this information. The map provides an interpretation of conductors in terms of length, strike and dip, geometric shape, conductance, depth, and thickness. The accuracy is comparable to an interpretation from a high quality ground EM survey having the same line spacing.

The appended EM anomaly list provides a tabulation of anomalies in ppm, conductance, and depth for the vertical sheet model. No conductance or depth estimates are shown for weak anomalous responses that are not of sufficient amplitude to yield reliable calculations.

Since discrete bodies normally are the targets of EM surveys, local base (or zero) levels are used to compute local anomaly amplitudes. This contrasts with the use of true zero levels which are used to compute true EM amplitudes. Local anomaly amplitudes are shown in the EM anomaly list and these are used to compute the vertical sheet parameters of conductance and depth.

Questionable Anomalies

The EM maps may contain anomalous responses that are displayed as asterisks (*). These responses denote weak anomalies of indeterminate conductance, which may reflect one of the following: a weak conductor near the surface, a strong conductor at depth (e.g., 100 to 120 m below surface) or to one side of the flight line, or aerodynamic noise. Those responses that have the appearance of valid bedrock anomalies on the flight profiles are indicated by appropriate interpretive symbols (see EM legend on maps). The others probably do not warrant further investigation unless their locations are of considerable geological interest.

The Thickness Parameter

A comparison of coaxial and coplanar shapes can provide an indication of the thickness of a steeply dipping conductor. The amplitude of the coplanar anomaly (e.g., CPI channel) increases relative to the coaxial anomaly (e.g., CXI) as the apparent thickness increases, i.e., the thickness in the horizontal plane. (The thickness is equal to the conductor width if the conductor dips at 90 degrees and strikes at right angles to the flight line.) This report refers to a conductor as thin when the thickness is likely to be less than 3 m, and thick when in excess of 10 m. Thick conductors are indicated on the EM map by parentheses "( )". For base metal exploration in steeply dipping geology, thick conductors can be high priority targets because many massive sulphide ore bodies are thick. The system cannot sense the thickness when the strike of the conductor is subparallel to the flight line, when the conductor has a shallow dip, when the anomaly amplitudes are small, or when the resistivity of the environment is below 100 ohm-m.

Resistivity Mapping

Resistivity mapping is useful in areas where broad or flat lying conductive units are of interest. One example of this is the clay alteration which is associated with Carlin-type deposits in the south west United States. The resistivity parameter was able to identify the clay alteration zone over the Cove deposit. The alteration zone appeared as a strong resistivity low on the 900 Hz resistivity parameter. The 7,200 Hz and 56,000 Hz resistivities showed more detail in the covering sediments, and delineated a range front fault. This is typical in many areas of the south west United States, where conductive near surface sediments, which may sometimes be alkalic, attenuate the higher frequencies.

Resistivity mapping has proven successful for locating diatremes in diamond exploration. Weathering products from relatively soft kimberlite pipes produce a resistivity contrast with the unaltered host rock. In many cases weathered kimberlite pipes were associated with thick conductive layers that contrasted with overlying or adjacent relatively thin layers of lake bottom sediments or overburden.

Areas of widespread conductivity are commonly encountered during surveys. These conductive zones may reflect alteration zones, shallow-dipping sulphide or graphite-rich units, saline ground water, or conductive overburden. In such areas, EM amplitude changes can be generated by decreases of only 5 m in survey altitude, as well as by increases in conductivity. The typical flight record in conductive areas is characterized by in-phase and quadrature channels that are continuously active. Local EM peaks reflect either increases in conductivity of the earth or decreases in survey altitude. For such conductive areas, apparent resistivity profiles and contour maps are necessary for the correct interpretation of the airborne data. The advantage of the resistivity parameter is that anomalies caused by altitude changes are virtually eliminated, so the resistivity data reflect only those anomalies caused by conductivity changes. The resistivity analysis also helps the interpreter to differentiate between conductive bedrock and conductive overburden. For example, discrete conductors will generally appear as narrow lows on the contour map and broad conductors (e.g., overburden) will appear as wide lows.

The apparent resistivity is calculated using the pseudo-layer (or buried) half-space model defined by Fraser (1978)[6]. This model consists of a resistive layer overlying a conductive half-space. The depth channels give the apparent depth below surface of the conductive material. The apparent depth is simply the apparent thickness of the overlying resistive layer. The apparent depth (or thickness) parameter will be positive when the upper layer is more resistive than the underlying material, in which case the apparent depth may be quite close to the true depth.

The apparent depth will be negative when the upper layer is more conductive than the underlying material, and will be zero when a homogeneous half-space exists. The apparent depth parameter must be interpreted cautiously because it will contain any errors that might exist in the measured altitude of the EM bird (e.g., as caused by a dense tree cover). The inputs to the resistivity algorithm are the in-phase and quadrature components of the coplanar coil-pair. The outputs are the apparent resistivity of the conductive half-space (the

---

6 Resistivity mapping with an airborne multicoil electromagnetic system: Geophysics, v. 43, p.144-172

source) and the sensor-source distance. The flying height is not an input variable, and the output resistivity and sensor-source distance are independent of the flying height when the conductivity of the measured material is sufficient to yield significant in-phase as well as quadrature responses. The apparent depth, discussed above, is simply the sensor-source distance minus the measured altitude or flying height. Consequently, errors in the measured altitude will affect the apparent depth parameter but not the apparent resistivity parameter.

The apparent depth parameter is a useful indicator of simple layering in areas lacking a heavy tree cover. Depth information has been used for permafrost mapping, where positive apparent depths were used as a measure of permafrost thickness. However, little quantitative use has been made of negative apparent depths because the absolute value of the negative depth is not a measure of the thickness of the conductive upper layer and, therefore, is not meaningful physically. Qualitatively, a negative apparent depth estimate usually shows that the EM anomaly is caused by conductive overburden. Consequently, the apparent depth channel can be of significant help in distinguishing between overburden and bedrock conductors.

Interpretation in Conductive Environments

Environments having low background resistivities (e.g., below 30 ohm-m for a 900 Hz system) yield very large responses from the conductive ground. This usually prohibits the recognition of discrete bedrock conductors. However, Fugro data processing techniques produce three parameters that contribute significantly to the recognition of bedrock conductors in conductive environments. These are the in-phase and quadrature difference channels (DIFI and DIFQ, which are available only on systems with "common" frequencies on orthogonal coil pairs), and the resistivity and depth channels (RES and DEP) for each coplanar frequency.

The EM difference channels (DIFI and DIFQ) eliminate most of the responses from conductive ground, leaving responses from bedrock conductors, cultural features (e.g., telephone lines, fences, etc.) and edge effects. Edge effects often occur near the perimeter of broad conductive zones. This can be a source of geologic noise. While edge effects yield anomalies on the EM difference channels, they do not produce resistivity anomalies. Consequently, the resistivity channel aids in eliminating anomalies due to edge effects. On the other hand, resistivity anomalies will coincide with the most highly conductive sections of conductive ground, and this is another source of geologic noise. The recognition of a bedrock conductor in a conductive environment therefore is based on the anomalous responses of the two difference channels (DIFI and DIFQ) and the resistivity channels (RES). The most favourable situation is where anomalies coincide on all channels.

The DEP channels, which give the apparent depth to the conductive material, also help to determine whether a conductive response arises from surficial material or from a conductive zone in the bedrock. When these channels ride above the zero level on the depth profiles (i.e., depth is negative), it implies that the EM and resistivity profiles are responding primarily to a conductive upper layer, i.e., conductive overburden. If the DEP channels are below the zero level, it indicates that a resistive upper layer exists, and this usually implies the existence of a bedrock conductor. If the low frequency DEP channel is below the zero level and the high frequency DEP is above, this suggests that a bedrock conductor occurs beneath conductive cover.

Reduction of Geologic Noise

Geologic noise refers to unwanted geophysical responses. For purposes of airborne EM surveying, geologic noise refers to EM responses caused by conductive overburden and magnetic permeability. It was mentioned previously that the EM difference channels (i.e., channel DIFI for in-phase and DIFQ for quadrature) tend to eliminate the response of conductive overburden.

Magnetite produces a form of geological noise on the in-phase channels. Rocks containing less than 1% magnetite can yield negative in-phase anomalies caused by magnetic permeability. When magnetite is widely distributed throughout a survey area, the in-phase EM channels may continuously rise and fall, reflecting variations in the magnetite percentage, flying height, and overburden thickness. This can lead to difficulties in recognizing deeply buried bedrock conductors, particularly if conductive overburden also exists. However, the response of broadly distributed magnetite generally vanishes on the in-phase difference channel DIFI. This feature can be a significant aid in the recognition of conductors that occur in rocks containing accessory magnetite.

EM Magnetite Mapping

The information content of HEM data consists of a combination of conductive eddy current responses and magnetic permeability responses. The secondary field resulting from conductive eddy current flow is frequency-dependent and consists of both in-phase and quadrature components, which are positive in sign. On the other hand, the secondary field resulting from magnetic permeability is independent of frequency and consists of only an in-phase component which is negative in sign. When magnetic permeability manifests itself by decreasing the measured amount of positive in-phase, its presence may be difficult to recognize. However, when it manifests itself by yielding a negative in-phase anomaly (e.g., in the absence of eddy current flow), its presence is assured. In this latter case, the negative component can be used to estimate the percent magnetite content.

A magnetite mapping technique, based on the low frequency coplanar data, can be complementary to magnetometer mapping in certain cases. Compared to magnetometry, it is far less sensitive but is more able to resolve closely spaced magnetite zones, as well as providing an estimate of the amount of magnetite in the rock. The method is sensitive to 1/4% magnetite by weight when the EM sensor is at a height of 30 m above a magnetitic half-space. It can individually resolve steep dipping narrow magnetite-rich bands which are separated by 60 m. Unlike magnetometry, the EM magnetite method is unaffected by remanent magnetism or magnetic latitude.

The EM magnetite mapping technique provides estimates of magnetite content which are usually correct within a factor of 2 when the magnetite is fairly uniformly distributed. EM magnetite maps can be generated when magnetic permeability is evident as negative in-phase responses on the data profiles.

Like magnetometry, the EM magnetite method maps only bedrock features, provided that the overburden is characterized by a general lack of magnetite. This contrasts with resistivity mapping which portrays the combined effect of bedrock and overburden.

The Susceptibility Effect

When the host rock is conductive, the positive conductivity response will usually dominate the secondary field, and the susceptibility effect[7] will appear as a reduction in the in-phase, rather than as a negative value. The in-phase response will be lower than would be predicted by a model using zero susceptibility. At higher frequencies the in-phase conductivity response also gets larger, so a negative magnetite effect observed on the low frequency might not be observable on the higher frequencies, over the same body. The susceptibility effect is most obvious over discrete magnetite-rich zones, but also occurs over uniform geology such as a homogeneous half-space.

High magnetic susceptibility will affect the calculated apparent resistivity, if only conductivity is considered. Standard apparent resistivity algorithms use a homogeneous half-space model, with zero susceptibility. For these algorithms, the reduced in-phase response will, in most cases, make the apparent resistivity higher than it should be. It is important to note that there is nothing wrong with the data, nor is there anything wrong with the processing algorithms. The apparent difference results from the fact that the simple geological model used in processing does not match the complex geology.

Measuring and Correcting the Magnetite Effect

Theoretically, it is possible to calculate (forward model) the combined effect of electrical conductivity and magnetic susceptibility on an EM response in all environments. The difficulty lies, however, in separating out the susceptibility effect from other geological effects when deriving resistivity and susceptibility from EM data.

Over a homogeneous half-space, there is a precise relationship between in-phase, quadrature, and altitude. These are often resolved as phase angle, amplitude, and altitude. Within a reasonable range, any two of these three parameters can be used to calculate the half space resistivity. If the rock has a positive magnetic susceptibility, the in-phase component will be reduced and this departure can be recognized by comparison to the other parameters.

---

7 Magnetic susceptibility and permeability are two measures of the same physical property. Permeability is generally given as relative permeability, μ_r, which is the permeability of the substance divided by the permeability of free space ($4\ \pi \times 10^{-7}$). Magnetic susceptibility k is related to permeability by $k=\mu^r-1$. Susceptibility is a unitless measurement, and is usually reported in units of 10^{-6}. The typical range of susceptibilities is –1 for quartz, 130 for pyrite, and up to 5×10^5 for magnetite, in 10^{-6} units (Telford et al, 1986).

The algorithm used to calculate apparent susceptibility and apparent resistivity from HEM data, uses a homogeneous half-space geological model. Non half-space geology, such as horizontal layers or dipping sources, can also distort the perfect half-space relationship of the three data parameters. While it may be possible to use more complex models to calculate both rock parameters, this procedure becomes very complex and time-consuming. For basic HEM data processing, it is most practical to stick to the simplest geological model.

Magnetite reversals (reversed in-phase anomalies) have been used for many years to calculate an "FeO" or magnetite response from HEM data (Fraser, 1981). However, this technique could only be applied to data where the in-phase was observed to be negative, which happens when susceptibility is high and conductivity is low.

Applying Susceptibility Corrections

Resistivity calculations done with susceptibility correction may change the apparent resistivity. High-susceptibility conductors, that were previously masked by the susceptibility effect in standard resistivity algorithms, may become evident. In this case the susceptibility corrected apparent resistivity is a better measure of the actual resistivity of the earth. However, other geological variations, such as a deep resistive layer, can also reduce the in-phase by the same amount. In this case, susceptibility correction would not be the best method. Different geological models can apply in different areas of the same data set. The effects of susceptibility, and other effects that can create a similar response, must be considered when selecting the resistivity algorithm.

Susceptibility from EM vs Magnetic Field Data

The response of the EM system to magnetite may not match that from a magnetometer survey. First, HEM-derived susceptibility is a rock property measurement, like resistivity. Magnetic data show the total magnetic field, a measure of the potential field, not the rock property. Secondly, the shape of an anomaly depends on the shape and direction of the source magnetic field. The electromagnetic field of HEM is much different in shape from the earth's magnetic field. Total field magnetic anomalies are different at different magnetic latitudes; HEM susceptibility anomalies have the same shape regardless of their location on the earth.

In far northern latitudes, where the magnetic field is nearly vertical, the total magnetic field measurement over a thin vertical dike is very similar in shape to the anomaly from the HEM-derived susceptibility (a sharp peak over the body). The same vertical dike at the magnetic equator would yield a negative magnetic anomaly, but the HEM susceptibility anomaly would show a positive susceptibility peak.

Effects of Permeability and Dielectric Permittivity

Resistivity algorithms that assume free-space magnetic permeability and dielectric permittivity, do not yield reliable values in highly magnetic or highly resistive areas. Both magnetic polarization and displacement currents cause a decrease in the in-phase component, often resulting in negative values that yield erroneously high apparent resistivities. The effects of magnetite occur at all frequencies, but are most evident at the lowest frequency. Conversely, the negative effects of dielectric permittivity are most evident at the higher frequencies, in resistive areas.

The table below shows the effects of varying permittivity over a resistive (10,000 ohm-m) half space, at frequencies of 56,000 Hz (DIGHEM^V) and 102,000 Hz (RESOLVE).

Apparent Resistivity Calculations
Effects of Permittivity on In-phase/Quadrature/Resistivity

Freq (Hz)	Coil	Sep (m)	Thres (ppm)	Alt (m)	In Phase	Quad Phase	App Res	App Depth (m)	Permittivity
56,000	CP	6.3	0.1	30	7.3	35.3	10118	-1.0	1 Air
56,000	CP	6.3	0.1	30	3.6	36.6	19838	-13.2	5 Quartz
56,000	CP	6.3	0.1	30	-1.1	38.3	81832	-25.7	10 Epidote
56,000	CP	6.3	0.1	30	-10.4	42.3	76620	-25.8	20 Granite
56,000	CP	6.3	0.1	30	-19.7	46.9	71550	-26.0	30 Diabase
56,000	CP	6.3	0.1	30	-28.7	52.0	66787	-26.1	40 Gabbro
102,000	CP	7.86	0.1	30	32.5	117.2	9409	-0.3	1 Air
102,000	CP	7.86	0.1	30	11.7	127.2	25956	-16.8	5 Quartz
102,000	CP	7.86	0.1	30	-14.0	141.6	97064	-26.5	10 Epidote
102,000	CP	7.86	0.1	30	-62.9	176.0	83995	-26.8	20 Granite
102,000	CP	7.86	0.1	30	-107.5	215.8	73320	-27.0	30 Diabase
102,000	CP	7.86	0.1	30	-147.1	259.2	64875	-27.2	40 Gabbro

Methods have been developed (Huang and Fraser, 2000, 2001) to correct apparent resistivities for the effects of permittivity and permeability. The corrected resistivities yield more credible values than if the effects of permittivity and permeability are disregarded.

Recognition of Culture

Cultural responses include all EM anomalies caused by man-made metallic objects. Such anomalies may be caused by inductive coupling or current gathering. The concern of the interpreter is to recognize when an EM response is due to culture. Points of consideration used by the interpreter, when coaxial and coplanar coil-pairs are operated at a common frequency, are as follows:

1. Channels CXPL and CPPL monitor 60 Hz radiation. An anomaly on these channels shows that the conductor is radiating power. Such an indication is normally a guarantee that the conductor is cultural. However, care must be taken to ensure that the conductor is not a geologic body that strikes across a power line, carrying leakage currents.

2. A flight that crosses a "line" (e.g., fence, telephone line, etc.) yields a centre-peaked coaxial anomaly and an m-shaped coplanar anomaly.[8] When the flight crosses the cultural line at a high angle of intersection, the amplitude ratio of coaxial/coplanar response is 2. Such an EM anomaly can only be caused by a line. The geologic body that yields anomalies most closely resembling a line is the vertically dipping thin dike. Such a body, however, yields an amplitude ratio of 1 rather than 2. Consequently, an m-shaped coplanar anomaly with a CXI/CPI amplitude ratio of 2 is virtually a guarantee that the source is a cultural line.

3. A flight that crosses a sphere or horizontal disk yields centre-peaked coaxial and coplanar anomalies with a CXI/CPI amplitude ratio (i.e., coaxial/coplanar) of 1/8. In the absence of geologic bodies of this geometry, the most likely conductor is a metal roof or small fenced yard.[9] Anomalies of this type are virtually certain to be cultural if they occur in an area of culture.

4. A flight that crosses a horizontal rectangular body or wide ribbon yields an m-shaped coaxial anomaly and a centre-peaked coplanar anomaly. In the absence of geologic bodies of this geometry, the most likely conductor is a large fenced area.[5] Anomalies of this type are virtually certain to be cultural if they occur in an area of culture.

5. EM anomalies that coincide with culture, as seen on the camera film or video display, are usually caused by culture. However, care is taken with such coincidences because a geologic conductor could occur beneath a fence, for example. In this example, the fence would be expected to yield an m-shaped coplanar anomaly as in case #2 above. If, instead, a centre-peaked coplanar anomaly occurred, there would be concern that a thick geologic conductor coincided with the cultural line.

6. The above description of anomaly shapes is valid when the culture is not conductively coupled to the environment. In this case, the anomalies arise from inductive coupling to the EM transmitter. However, when the environment is quite conductive (e.g., less than 100 ohm-m at 900 Hz), the cultural conductor may be conductively coupled to the environment. In this latter case, the anomaly shapes tend to be governed by current gathering. Current gathering can completely distort

---

8 See Figure C-1 presented earlier.

9 It is a characteristic of EM that geometrically similar anomalies are obtained from: (1) a planar conductor, and (2) a wire which forms a loop having dimensions identical to the perimeter of the equivalent planar conductor.

the anomaly shapes, thereby complicating the identification of cultural anomalies. In such circumstances, the interpreter can only rely on the radiation channels and on the camera film or video records.

Magnetic Responses

The measured total magnetic field provides information on the magnetic properties of the earth materials in the survey area. The information can be used to locate magnetic bodies of direct interest for exploration, and for structural and lithological mapping.

The total magnetic field response reflects the abundance of magnetic material in the source. Magnetite is the most common magnetic mineral. Other minerals such as ilmenite, pyrrhotite, franklinite, chromite, hematite, arsenopyrite, limonite and pyrite are also magnetic, but to a lesser extent than magnetite on average.

In some geological environments, an EM anomaly with magnetic correlation has a greater likelihood of being produced by sulphides than one which is non-magnetic. However, sulphide ore bodies may be non-magnetic (e.g., the Kidd Creek deposit near Timmins, Canada) as well as magnetic (e.g., the Mattabi deposit near Sturgeon Lake, Canada).

Iron ore deposits will be anomalously magnetic in comparison to surrounding rock due to the concentration of iron minerals such as magnetite, ilmenite and hematite.

Changes in magnetic susceptibility often allow rock units to be differentiated based on the total field magnetic response. Geophysical classifications may differ from geological classifications if various magnetite levels exist within one general geological classification. Geometric considerations of the source such as shape, dip and depth, inclination of the earth's field and remanent magnetization will complicate such an analysis.

In general, mafic lithologies contain more magnetite and are therefore more magnetic than many sediments which tend to be weakly magnetic. Metamorphism and alteration can also increase or decrease the magnetization of a rock unit.

Textural differences on a total field magnetic contour, colour or shadow map due to the frequency of activity of the magnetic parameter resulting from inhomogeneities in the distribution of magnetite within the rock, may define certain lithologies. For example, near surface volcanics may display highly complex contour patterns with little line-to-line correlation.

Rock units may be differentiated based on the plan shapes of their total field magnetic responses. Mafic intrusive plugs can appear as isolated "bulls-eye" anomalies. Granitic intrusives appear as sub-circular zones, and may have contrasting rings due to contact metamorphism. Generally, granitic terrain will lack a pronounced strike direction, although granite gneiss may display strike.

Linear north-south units are theoretically not well-defined on total field magnetic maps in equatorial regions due to the low inclination of the earth's magnetic field. However, most stratigraphic units will have variations in composition along strike that will cause the units to appear as a series of alternating magnetic highs and lows.

Faults and shear zones may be characterized by alteration that causes destruction of magnetite (e.g., weathering) that produces a contrast with surrounding rock. Structural breaks may be filled by magnetite-rich, fracture filling material as is the case with diabase dikes, or by non-magnetic felsic material.

Faulting can also be identified by patterns in the magnetic total field contours or colours. Faults and dikes tend to appear as lineaments and often have strike lengths of several kilometres. Offsets in narrow, magnetic, stratigraphic trends also delineate structure. Sharp contrasts in magnetic lithologies may arise due to large displacements along strike-slip or dip-slip faults.

APPENDIX D

DATA ARCHIVE DESCRIPTION

APPENDIX D

ARCHIVE DESCRIPTION

```
Reference: CCD02424
# of CD's: 1
Archive Date: April 3, 2006

--------------------------------------------------------------------------------
This archive contains final data archives and grids of an airborne geophysical
survey conducted by FUGRO AIRBORNE SURVEYS CORP. on behalf of Strongbow Exploration Inc.
during January, 2006.

Job # 06004

--------------------------------------------------------------------------------

This CD consists of an encrypted file containing 30 files in 5 directories

******* Disc 1 of 1 *******

\GRIDS
        Grids in Geosoft binary float (.GRD) format

      MAG                      - Total Magnetic Field
      CVG                      - Calculated Vertical Magnetic Gradient
      RES900                   - Apparent Resistivity 900 Hz coplanar
      RES7200                  - Apparent Resistivity 7200 Hz coplanar
      RES56K                   - Apparent Resistivity 56000 Hz coplanar

\LINEDATA
      SKOONKACREEK.TXT         - Documentation for data archive file
      SKOONKACREEK.XYZ         - Final data archive in Geosoft XYZ format
      ANOMALY.TXT              - Documentation for data archive file
      ANOMALY.XYZ              - Final data archive in Geosoft XYZ format

\REPORT
        SKOONKACREEK.PDF       - Logistics and Interpretation Report
        SKOONKACREEK.DOC       - Logistics and Interpretation Report in MS-Word

\HPGL2
        files created with HP Designjet 5500 printer driver v5.32

      ANOM_*.PRN               - Electromagnetic Anomalies
      CVG_*.PRN                - Calculated Vertical Magnetic Gradient, Colour
      MAG_*.PRN                - Total Field Magnetics, Colour
      R72_*.PRN                - 7200 Hz Apparent Resistivity, Colour
      R56_*.PRN                - 7200 Hz Apparent Resistivity, Colour
      BW_CVG_*.PRN             - Calculated Vertical Magnetic Gradient, Black and White
      BW_MAG_*.PRN             - Total Field Magnetics, Black and White
      BW_R72_*.PRN             - 7200 Hz Apparent Resistivity, Black and White
      BW_R56_*.PRN             - 7200 Hz Apparent Resistivity, Black and White

      where * is the map scale 10000 or 7500.
```

\VECTORS (in AutoCAD R13)
ANOM.DWG - Electromagnetic Anomalies

The coordinate system for all grids and the data archive is projected as follows

Datum	NAD83
Spheroid	GRS 80
Projection	UTM
Central meridian	123 West (Z10N)
False easting	500000
False northing	0
Scale factor	0.9996
Northern parallel	N/A
Base parallel	N/A
WGS84 to local conversion method	Molodensky
Delta X shift	0
Delta Y shift	0
Delta Z shift	0

If you have any problems with this archive please contact

Processing Manager
FUGRO AIRBORNE SURVEYS CORP.
2270 Argentia Road, Unit 2
Mississauga, Ontario
Canada L5N 6A6
Tel (905) 812-0212
Fax (905) 812-1504
E-mail toronto@fugroairborne.com

Geosoft XYZ ARCHIVE SUMMARY

JOB # :06004
TYPE OF SURVEY :EM, MAGNETICS, RESISTIVITY, RADIOMETRICS
AREA :Skoonka Creek, British Columbia
CLIENT :Strongbow Exploration Inc.

****

NUMBER OF DATA FIELDS : 44

#	CHANNAME	TIME	UNITS	DESCRIPTION	# BYTES	decimal
1	X	0.10	m	UTME - NAD83 Zone 10	11	2
2	Y	0.10	m	UTMN - NAD83 Zone 10	11	2
3	FLT	0.10	n/a	Flight Number	6	0
4	DATE	0.10	YYYY/	Flight Date	9	1
5	FID	1.00	n/a	Synchronization Counter	9	2
6	ALTBIRDM	0.10	m	Em Bird to Earth-Surface, Radar Altimeter	9	2
7	GALT	0.10	m	GPS Height above ellipsoid	9	2
8	BARO	0.10	m	Barometric Altitude	9	2
9	MAG1U	0.10	nT	Uncorrected, Spike Rejected Magnetics	10	3
10	DIURNAL	0.10	nT	Daily Variations of Magnetic Field	10	3
11	DIU_COR	0.10	nT	Diurnal Correction Applied	10	3
12	MAG	0.10	nT	Final Leveled Total Magnetic Field	10	3
13	CPIR900	0.10	ppm	Uncorrected Inphase Coplanar 870 Hz	10	2
14	CPQR900	0.10	ppm	Uncorrected Quadrature Coplanar 870 Hz	10	2
15	CXIR1000	0.10	ppm	Uncorrected Inphase Coaxial 1112 Hz	10	2
16	CXQR1000	0.10	ppm	Uncorrected Quadrature Coaxial 1112 Hz	10	2
17	CXIR5500	0.10	ppm	Uncorrected Inphase Coaxial 5686 Hz	10	2
18	CXQR5500	0.10	ppm	Uncorrected Quadrature Coaxial 5686 Hz	10	2
19	CPIR7200	0.10	ppm	Uncorrected Inphase Coplanar 7300 Hz	10	2
20	CPQR7200	0.10	ppm	Uncorrected Quadrature Coplanar 7300 Hz	10	2
21	CPIR56K	0.10	ppm	Uncorrected Inphase Coplanar 55400 Hz	10	2
22	CPQR56K	0.10	ppm	Uncorrected Quadrature Coplanar 55400 Hz	10	2
23	CPI900	0.10	ppm	Inphase Coplanar 870 Hz	10	2
24	CPQ900	0.10	ppm	Quadrature Coplanar 870 Hz	10	2
25	CXI1000	0.10	ppm	Inphase Coaxial 1112 Hz	10	2
26	CXQ1000	0.10	ppm	Quadrature Coaxial 1112 Hz	10	2
27	CXI5500	0.10	ppm	Inphase Coaxial 5686 Hz	10	2
28	CXQ5500	0.10	ppm	Quadrature Coaxial 5686 Hz	10	2
29	CPI7200	0.10	ppm	Inphase Coplanar 7300 Hz	10	2
30	CPQ7200	0.10	ppm	Quadrature Coplanar 7300 Hz	10	2
31	CPI56K	0.10	ppm	Inphase Coplanar 55400 Hz	10	2
32	CPQ56K	0.10	ppm	Quadrature Coplanar 55400 Hz	10	2
33	RES900	0.10	ohm·m	Apparent Resistivity 870 Hz	10	2
34	RES7200	0.10	ohm·m	Apparent Resistivity 7300 Hz	10	2
35	RES56K	0.10	ohm·m	Apparent Resistivity 55400 Hz	10	2
36	DEP900	0.10	m	Apparent Depth 870 Hz	10	2
37	DEP7200	0.10	m	Apparent Depth 7300 Hz	10	2
38	DEP56K	0.10	m	Apparent Depth 55400 Hz	10	2
39	DIFI	0.10	n/a	Inphase Difference Channel	10	2
40	DIFQ	0.10	n/a	Quadrature Difference Channe	10	2
41	CDT	0.10	n/a	Conductivity Thickness	10	2
42	FLAG_MAG	0.10	n/a	Magnetics Spike Rejection Flag	10	2
43	QC_ALTDEVFLAG	0.10	n/a	Altitude Deviation Flag	10	2

```
 44 QC_FPDEVFLAG      0.10   n/a   Flight Path Deviation Flag                10      2
****************************************************************************************

ISSUE DATE          :April 3, 2006
FOR WHOM            :Strongbow Exploration Inc.
BY  WHOM            :Fugro Airborne Surveys Corp.
                     2270 Argentia Road, Unit 2
                     Mississauga, Ontario,
                     Canada  L5N 6A6
                     TEL. (905) 812-0212
                     FAX  (905) 812-1504
```

Geosoft XYZ ARCHIVE SUMMARY

JOB # :06004
TYPE OF SURVEY :EM, MAGNETICS, RESISTIVITY, RADIOMETRICS
AREA :Skoonka Creek, British Columbia
CLIENT :Strongbow Exploration Inc.

****

NUMBER OF DATA FIELDS : 44

#	CHANNAME	TIME	UNITS	DESCRIPTION	# BYTES	decimal
1	X	0.10	m	UTME - NAD83 Zone 10	11	2
2	Y	0.10	m	UTMN - NAD83 Zone 10	11	2
3	FLT	0.10	n/a	Flight Number	6	0
4	DATE	0.10	YYYY/	Flight Date	9	1
5	FID	1.00	n/a	Synchronization Counter	9	2
6	ALTBIRDM	0.10	m	Em Bird to Earth-Surface, Radar Altimeter	9	2
7	GALT	0.10	m	GPS Height above ellipsoid	9	2
8	BARO	0.10	m	Barometric Altitude	9	2
9	MAG1U	0.10	nT	Uncorrected, Spike Rejected Magnetics	10	3
10	DIURNAL	0.10	nT	Daily Variations of Magnetic Field	10	3
11	DIU_COR	0.10	nT	Diurnal Correction Applied	10	3
12	MAG	0.10	nT	Final Leveled Total Magnetic Field	10	3
13	CPIR900	0.10	ppm	Uncorrected Inphase Coplanar 870 Hz	10	2
14	CPQR900	0.10	ppm	Uncorrected Quadrature Coplanar 870 Hz	10	2
15	CXIR1000	0.10	ppm	Uncorrected Inphase Coaxial 1112 Hz	10	2
16	CXQR1000	0.10	ppm	Uncorrected Quadrature Coaxial 1112 Hz	10	2
17	CXIR5500	0.10	ppm	Uncorrected Inphase Coaxial 5686 Hz	10	2
18	CXQR5500	0.10	ppm	Uncorrected Quadrature Coaxial 5686 Hz	10	2
19	CPIR7200	0.10	ppm	Uncorrected Inphase Coplanar 7300 Hz	10	2
20	CPQR7200	0.10	ppm	Uncorrected Quadrature Coplanar 7300 Hz	10	2
21	CPIR56K	0.10	ppm	Uncorrected Inphase Coplanar 55400 Hz	10	2
22	CPQR56K	0.10	ppm	Uncorrected Quadrature Coplanar 55400 Hz	10	2
23	CPI900	0.10	ppm	Inphase Coplanar 870 Hz	10	2
24	CPQ900	0.10	ppm	Quadrature Coplanar 870 Hz	10	2
25	CXI1000	0.10	ppm	Inphase Coaxial 1112 Hz	10	2
26	CXQ1000	0.10	ppm	Quadrature Coaxial 1112 Hz	10	2
27	CXI5500	0.10	ppm	Inphase Coaxial 5686 Hz	10	2
28	CXQ5500	0.10	ppm	Quadrature Coaxial 5686 Hz	10	2
29	CPI7200	0.10	ppm	Inphase Coplanar 7300 Hz	10	2
30	CPQ7200	0.10	ppm	Quadrature Coplanar 7300 Hz	10	2
31	CPI56K	0.10	ppm	Inphase Coplanar 55400 Hz	10	2
32	CPQ56K	0.10	ppm	Quadrature Coplanar 55400 Hz	10	2
33	RES900	0.10	ohm·m	Apparent Resistivity 870 Hz	10	2
34	RES7200	0.10	ohm·m	Apparent Resistivity 7300 Hz	10	2
35	RES56K	0.10	ohm·m	Apparent Resistivity 55400 Hz	10	2
36	DEP900	0.10	m	Apparent Depth 870 Hz	10	2
37	DEP7200	0.10	m	Apparent Depth 7300 Hz	10	2
38	DEP56K	0.10	m	Apparent Depth 55400 Hz	10	2
39	DIFI	0.10	n/a	Inphase Difference Channel	10	2
40	DIFQ	0.10	n/a	Quadrature Difference Channe	10	2
41	CDT	0.10	n/a	Conductivity Thickness	10	2
42	FLAG_MAG	0.10	n/a	Magnetics Spike Rejection Flag	10	2
43	QC_ALTDEVFLAG	0.10	n/a	Altitude Deviation Flag	10	2

44 QC_FPDEVFLAG	0.10	n/a	Flight Path Deviation Flag	10	2

****

ISSUE DATE :April 3, 2006
FOR WHOM :Strongbow Exploration Inc.
BY WHOM :Fugro Airborne Surveys Corp.
2270 Argentia Road, Unit 2
Mississauga, Ontario,
Canada L5N 6A6
TEL. (905) 812-0212
FAX (905) 812-1504

APPENDIX E

EM ANOMALY LIST

EM Anomaly List

Label	Fid	Interp	XUTM m	YUTM m	CX 5500 HZ Real ppm	CX 5500 HZ Quad ppm	CP 7200 HZ Real ppm	CP 7200 HZ Quad ppm	CP 900 HZ Real ppm	CP 900 HZ Quad ppm	Vertical Dike COND siemens	Vertical Dike DEPTH* m	Mag. Corr NT
LINE 10010		FLIGHT 4											
A	8061.5	S	605049	5577741	15.1	18.5	99.1	130.2	3.4	33.3	1.2	14	221
B	8071.0	S	605046	5577981	12.1	13.9	135.4	82.0	19.4	43.7	1.2	0	0
C	8074.0	S?	605049	5578060	20.6	20.4	135.4	82.0	19.4	43.7	1.7	0	297
D	8100.8	S	605055	5578580	8.6	22.8	64.3	182.3	4.1	27.6	0.5	0	0
E	8112.7	S?	605050	5578919	0.0	16.7	39.7	14.9	12.5	8.6	---	---	205
F	8123.3	S	605054	5579242	14.5	15.4	78.9	114.2	41.9	22.6	1.4	12	0
G	8149.5	B?	605050	5579678	30.5	47.6	197.4	273.2	42.8	69.9	1.2	0	0
H	8155.7	S?	605048	5579810	21.2	22.2	22.0	67.9	42.8	6.8	1.6	11	0
I	8169.4	B?	605052	5580021	9.6	39.3	21.2	169.3	15.9	25.4	0.4	0	653
J	8180.2	B?	605058	5580206	15.8	72.4	106.9	448.1	76.8	70.4	0.4	0	47
K	8190.0	S?	605048	5580445	0.0	0.2	17.0	0.2	90.1	0.0	---	---	0
L	8194.0	H	605047	5580544	15.5	19.6	26.2	85.5	90.1	9.3	1.2	12	0
M	8207.5	S?	605049	5580804	3.3	17.2	42.9	196.7	8.4	18.1	0.2	0	0
N	8233.8	S	605053	5581174	10.0	23.4	25.4	101.0	17.8	11.2	0.6	0	0
O	8236.2	E	605051	5581226	6.8	28.1	25.4	101.0	24.6	11.2	0.3	0	299
P	8254.6	S	605052	5581653	6.6	23.5	80.6	121.3	12.0	35.5	0.3	4	56
Q	8271.8	S?	605063	5582042	8.1	17.8	73.2	85.0	7.1	22.3	0.5	17	0
LINE 10020		FLIGHT 3											
A	1812.5	S	605144	5577462	*	*	*	*	*	*	---	---	0
B	1795.4	B?	605149	5577894	33.2	34.1	210.3	215.3	13.3	71.7	1.9	0	330
C	1792.6	S	605145	5577967	17.0	19.6	210.3	215.3	13.3	71.7	1.3	2	330
D	1790.1	S	605142	5578033	21.4	21.7	210.3	156.8	38.0	71.7	1.6	0	0
E	1771.7	E	605148	5578469	16.1	41.4	69.0	135.5	24.9	10.3	0.6	0	639
F	1762.1	S?	605156	5578672	8.0	9.9	49.4	137.8	48.9	19.4	0.9	26	653
G	1747.7	S?	605149	5578971	1.0	14.1	1.7	64.5	15.4	8.1	---	---	0
H	1735.7	S	605146	5579236	18.3	22.2	113.7	188.8	31.4	36.6	1.3	11	0
I	1730.9	S?	605149	5579334	1.6	27.8	112.2	321.1	31.4	55.7	---	---	262
J	1727.5	B	605147	5579388	11.4	36.9	30.3	321.1	3.2	55.7	0.5	3	0
K	1715.7	S?	605146	5579566	20.4	69.4	222.8	393.3	18.0	70.3	0.5	0	0
L	1710.5	S	605152	5579686	17.7	12.0	222.8	393.3	17.2	70.3	2.5	14	0
M	1691.3	S?	605155	5580021	0.8	7.9	8.9	97.4	9.8	12.0	---	---	821
N	1666.4	S	605136	5580339	12.9	27.5	92.1	164.8	8.1	37.6	0.7	0	0
O	1658.4	B	605141	5580479	40.3	65.9	121.8	142.2	15.7	43.8	1.2	9	0
P	1648.8	E	605154	5580640	6.7	6.0	47.2	36.6	27.0	8.3	1.3	24	0
Q	1627.1	S?	605145	5580909	4.8	22.2	20.8	137.0	2.5	18.0	0.3	0	0
R	1613.2	S	605142	5581025	3.0	4.9	22.1	80.6	14.7	9.9	---	---	0

CX = COAXIAL
CP = COPLANAR

Note:EM values shown above are local amplitudes

*Estimated Depth may be unreliable because the stronger part of the conductor may be deeper or to one side of the flight line, or because of a shallow dip or magnetite/overburden effects

EM Anomaly List

Label	Fid	Interp	XUTM m	YUTM m	CX 5500 HZ Real ppm	CX 5500 HZ Quad ppm	CP 7200 HZ Real ppm	CP 7200 HZ Quad ppm	CP 900 HZ Real ppm	CP 900 HZ Quad ppm	Vertical Dike COND siemens	Vertical Dike DEPTH* m	Mag. Corr NT
LINE 10020			FLIGHT 3										
S	1602.9	S	605150	5581132	12.2	17.8	64.7	130.1	25.2	21.4	0.9	0	0
T	1576.2	S?	605149	5581595	0.1	20.9	41.7	92.4	36.9	15.5	---	---	378
U	1559.0	S	605147	5581899	9.1	11.6	58.1	78.3	7.3	20.1	1.0	23	0
V	1550.0	S	605147	5582097	12.9	14.4	63.0	28.9	2.7	16.8	1.2	16	0
LINE 10030			FLIGHT 3										
A	1911.3	S	605257	5577484	42.0	44.8	266.6	406.3	1.1	84.2	1.9	0	0
B	1918.4	S?	605257	5577639	16.7	40.1	177.1	260.3	12.7	57.5	0.7	0	0
C	1944.5	D	605252	5577983	12.0	21.9	47.1	89.6	2.8	19.6	0.7	6	248
D	1957.4	E	605262	5578204	57.9	78.3	485.5	546.0	31.0	147.7	1.7	0	0
E	1962.0	S?	605267	5578297	66.0	72.6	485.5	546.0	31.0	147.7	2.2	0	0
F	1971.9	B?	605260	5578425	13.8	26.4	118.6	103.5	16.3	10.5	0.7	7	88
G	1979.1	S	605257	5578479	9.4	11.0	118.6	131.3	24.1	28.5	1.1	29	0
H	2025.5	S?	605260	5579250	38.2	22.4	160.1	132.6	40.9	36.0	3.8	6	0
I	2035.0	S	605252	5579526	7.1	0.6	78.8	64.0	17.1	15.0	---	---	0
J	2038.7	S	605248	5579640	13.8	20.3	78.8	64.0	17.1	14.6	1.0	12	143
K	2047.9	S?	605244	5579901	8.0	14.2	30.7	110.7	12.1	13.9	0.7	11	831
L	2061.0	S?	605251	5580293	5.1	1.2	9.8	44.4	20.0	8.7	---	---	86
M	2072.1	E	605247	5580651	6.0	24.5	61.2	164.8	47.0	16.8	0.3	0	0
N	2075.1	S?	605246	5580714	1.6	22.4	61.2	164.8	32.0	16.8	---	---	0
O	2086.2	S?	605247	5580863	2.7	38.2	23.2	201.3	50.9	26.1	---	---	0
P	2100.4	S?	605252	5581093	15.2	12.9	60.1	21.4	38.9	7.9	1.8	5	0
Q	2105.8	S?	605255	5581213	0.2	23.2	30.5	174.7	0.2	26.3	---	---	0
R	2122.8	S?	605252	5581559	0.0	16.1	3.5	50.4	9.8	5.5	---	---	626
S	2139.7	S?	605245	5581904	7.4	10.1	51.9	41.0	9.3	13.9	0.8	13	0
LINE 10040			FLIGHT 3										
A	2427.2	S	605347	5577610	21.6	26.3	165.9	336.1	16.7	58.2	1.3	0	0
B	2411.2	D	605354	5578017	21.5	25.2	70.0	93.8	0.3	22.6	1.4	7	0
C	2394.9	S	605337	5578319	44.8	86.0	563.3	615.5	28.3	191.4	1.1	0	0
D	2392.7	S	605337	5578371	63.8	100.3	563.3	615.5	64.9	191.4	1.5	0	0
E	2385.5	E	605344	5578526	31.8	46.8	271.7	348.7	62.7	76.5	1.3	2	548
F	2364.0	S?	605351	5579037	6.2	20.1	34.2	144.6	26.7	15.6	0.4	1	0
G	2355.3	S	605345	5579289	18.5	15.6	169.2	73.7	38.1	29.7	1.9	9	0
H	2351.9	S?	605345	5579385	18.2	27.5	169.2	73.7	35.8	29.7	1.0	12	0
I	2343.7	S	605350	5579622	7.8	16.6	31.7	62.7	8.2	12.3	0.6	11	0
J	2323.8	S?	605352	5580115	152.3	382.3	1025.3	1914.5	16.7	329.5	1.3	0	382
K	2295.0	S?	605340	5580779	7.9	18.7	30.0	80.6	6.2	12.0	0.5	3	150

CX = COAXIAL
CP = COPLANAR

Note:EM values shown above are local amplitudes

*Estimated Depth may be unreliable because the stronger part of the conductor may be deeper or to one side of the flight line, or because of a shallow dip or magnetite/overburden effects

EM Anomaly List

Label	Fid	Interp	XUTM m	YUTM m	CX 5500 HZ Real ppm	CX 5500 HZ Quad ppm	CP 7200 HZ Real ppm	CP 7200 HZ Quad ppm	CP 900 HZ Real ppm	CP 900 HZ Quad ppm	Vertical Dike COND siemens	Vertical Dike DEPTH* m	Mag. Corr NT
LINE 10040			FLIGHT 3										
L	2260.2	E	605355	5581453	8.7	29.9	79.4	185.8	5.0	25.7	0.4	6	645
M	2225.1	S	605350	5582004	2.7	0.3	46.0	60.0	10.9	15.2	---	---	0
LINE 10050			FLIGHT 3										
A	2514.7	S	605448	5577750	25.6	32.5	235.2	263.9	24.3	69.7	1.4	0	0
B	2532.9	B?	605453	5578038	15.7	13.4	33.4	90.7	16.5	15.2	1.8	20	0
C	2554.0	S?	605458	5578364	34.9	16.2	318.8	208.2	30.5	104.0	5.1	14	0
D	2578.5	S?	605446	5578913	20.3	46.8	167.0	296.2	28.6	44.3	0.7	0	24
E	2595.5	B?	605452	5579431	12.9	7.8	125.6	84.9	22.1	23.4	2.6	24	0
F	2617.0	S?	605456	5580081	47.6	98.0	490.9	738.4	22.2	150.1	1.1	0	484
G	2660.0	S?	605451	5581339	9.5	25.5	176.5	349.6	17.1	55.4	0.5	0	155
H	2664.4	S?	605455	5581449	19.4	72.4	176.5	349.6	34.9	55.4	0.5	0	463
I	2703.7	B?	605446	5582220	31.9	81.4	56.5	206.3	0.0	25.6	0.8	0	0
LINE 10060			FLIGHT 3										
A	3046.5	E	605545	5577678	105.9	162.7	469.2	797.9	45.4	140.9	1.8	0	107
B	3041.5	S?	605544	5577792	29.8	72.8	469.2	385.5	56.1	130.7	0.8	0	0
C	3028.9	E	605540	5578051	13.3	13.1	110.8	87.6	8.8	30.7	1.4	13	0
D	3007.4	E	605550	5578385	13.0	31.2	206.1	138.2	32.9	71.2	0.6	6	0
E	3003.9	S	605551	5578470	35.0	20.4	206.1	118.7	32.9	71.2	3.8	1	250
F	2989.9	S	605546	5578783	28.7	26.6	197.4	194.3	38.3	51.1	2.0	1	0
G	2984.4	S?	605545	5578920	45.4	11.0	267.2	286.5	38.2	81.6	13.7	0	192
H	2980.0	S?	605546	5579042	12.3	31.3	267.2	286.5	7.9	81.6	0.6	0	0
I	2963.6	S	605547	5579502	20.3	31.4	154.9	229.2	15.1	43.7	1.0	0	0
J	2938.3	S?	605548	5580112	20.8	110.5	224.4	597.3	0.8	98.7	0.4	0	0
K	2888.1	B?	605545	5581351	26.5	64.8	299.0	516.2	46.1	78.2	0.8	0	68
L	2884.0	S?	605546	5581430	31.7	84.6	299.0	516.2	40.7	78.2	0.7	0	186
M	2865.1	S?	605551	5581716	0.0	22.7	8.4	153.2	3.8	18.8	---	---	0
N	2829.4	B?	605541	5582237	16.3	34.1	51.9	111.7	9.7	16.4	0.7	0	0
LINE 10070			FLIGHT 3										
A	3146.7	S	605650	5577770	111.8	104.3	544.1	505.0	78.6	177.5	3.1	0	0
B	3152.0	E	605657	5577894	37.4	35.7	266.6	186.1	37.9	7.7	2.1	7	163
C	3164.3	S?	605662	5578067	0.0	26.7	34.6	253.5	16.0	30.9	---	---	0
D	3178.4	S?	605666	5578136	0.0	45.5	30.0	179.6	0.0	22.2	---	---	81
E	3223.7	S?	605653	5578533	213.8	251.6	909.8	842.2	65.4	289.7	3.0	0	0
F	3225.7	S?	605652	5578591	86.3	251.6	909.8	842.2	63.4	289.7	1.0	0	0
G	3254.4	S	605654	5579522	14.0	16.1	50.2	88.9	6.1	14.7	1.2	8	0

CX = COAXIAL
CP = COPLANAR

Note:EM values shown above are local amplitudes

*Estimated Depth may be unreliable because the stronger part of the conductor may be deeper or to one side of the flight line, or because of a shallow dip or magnetite/overburden effects

EM Anomaly List

Label	Fid	Interp	XUTM m	YUTM m	CX 5500 HZ Real ppm	CX 5500 HZ Quad ppm	CP 7200 HZ Real ppm	CP 7200 HZ Quad ppm	CP 900 HZ Real ppm	CP 900 HZ Quad ppm	Vertical Dike COND siemens	Vertical Dike DEPTH* m	Mag. Corr NT
LINE 10070		FLIGHT 3											
H	3276.7	S	605657	5580193	20.5	31.3	105.7	228.1	26.0	44.2	1.0	0	0
I	3282.3	S	605660	5580373	9.9	12.1	47.6	0.0	27.2	9.1	1.0	19	0
J	3311.5	S?	605646	5581146	20.5	20.8	196.3	68.3	31.0	23.7	1.6	14	0
K	3320.4	S?	605655	5581390	23.6	58.1	210.4	324.1	28.7	61.1	0.7	0	697
L	3346.4	S?	605658	5581876	3.8	12.7	8.1	82.5	2.1	14.4	0.3	9	0
M	3360.0	B	605652	5582051	11.2	46.0	72.2	202.9	17.3	35.9	0.4	0	0
N	3371.4	B?	605642	5582221	28.2	154.7	120.5	633.6	33.4	75.3	0.4	0	0
LINE 10080		FLIGHT 3											
A	3680.9	S?	605746	5577563	6.8	15.1	9.3	102.0	62.4	18.7	0.5	12	0
B	3668.7	S?	605734	5577757	90.9	129.4	401.3	526.8	26.7	141.6	1.8	0	0
C	3660.3	E	605737	5577927	13.3	18.3	47.7	32.3	60.0	12.4	1.0	19	113
D	3641.5	S?	605735	5578199	0.7	48.7	29.7	268.5	28.6	31.4	---	---	0
E	3621.0	E	605744	5578527	64.8	77.9	668.8	680.4	68.3	240.4	2.0	0	0
F	3617.5	S	605746	5578615	64.5	103.8	761.0	680.4	100.5	240.4	1.5	0	0
G	3613.4	S	605747	5578729	151.1	110.1	761.0	680.4	100.5	246.3	4.6	0	0
H	3593.7	S?	605748	5579156	12.1	23.3	66.2	142.1	6.7	27.8	0.7	1	0
I	3579.2	S	605752	5579575	22.7	41.8	69.5	110.8	18.4	16.0	0.9	4	0
J	3570.6	S?	605747	5579812	2.0	19.6	0.2	66.8	20.3	7.1	---	---	814
K	3560.2	S?	605740	5580057	9.3	44.4	62.4	180.2	56.8	32.8	0.3	0	359
L	3553.4	S?	605743	5580226	20.6	65.9	138.7	470.6	5.9	76.7	0.6	0	121
M	3532.8	S?	605750	5580774	11.2	49.9	72.7	245.8	5.5	39.7	0.3	0	858
N	3510.0	S?	605744	5581282	24.2	43.3	259.0	434.9	66.6	63.9	0.9	0	750
O	3506.5	S?	605744	5581362	22.0	75.5	259.0	434.9	7.4	63.9	0.5	0	746
P	3489.5	S?	605750	5581617	0.0	19.9	30.8	147.9	8.8	18.2	---	---	0
Q	3438.0	S?	605741	5582187	15.7	9.6	69.2	69.1	7.2	16.0	2.7	16	0
LINE 10090		FLIGHT 3											
A	3773.4	D	605854	5577656	21.9	65.0	90.3	287.9	14.6	37.5	0.6	0	226
B	3780.7	E	605857	5577868	8.1	24.5	107.3	164.8	16.9	42.8	0.4	0	0
C	3801.5	S?	605849	5578173	0.2	5.6	23.0	36.6	21.9	3.9	---	---	581
D	3817.7	E	605851	5578576	61.0	76.3	468.4	469.9	23.8	167.0	1.8	0	0
E	3824.0	S	605851	5578797	52.9	51.9	468.4	469.9	53.4	167.0	2.3	0	163
F	3854.1	S	605852	5579642	8.4	13.3	75.1	104.2	7.3	21.9	0.7	15	0
G	3875.5	S	605837	5580153	7.0	9.5	57.2	145.6	23.6	24.8	0.8	11	186
H	3881.0	S?	605841	5580328	3.9	43.1	36.4	201.9	28.5	35.2	0.1	0	43
I	3905.0	S	605856	5580955	7.1	29.8	32.7	113.2	7.5	18.1	0.3	2	0
J	3910.1	S?	605853	5581085	4.5	3.1	27.4	14.6	25.3	2.4	---	---	0

CX = COAXIAL
CP = COPLANAR

Note:EM values shown above are local amplitudes

*Estimated Depth may be unreliable because the stronger part of the conductor may be deeper or to one side of the flight line, or because of a shallow dip or magnetite/overburden effects

Label	Fid	Interp	XUTM m	YUTM m	CX 5500 HZ Real ppm	CX 5500 HZ Quad ppm	CP 7200 HZ Real ppm	CP 7200 HZ Quad ppm	CP 900 HZ Real ppm	CP 900 HZ Quad ppm	Vertical Dike COND siemens	Vertical Dike DEPTH* m	Mag. Corr NT
LINE 10090		FLIGHT 3											
K	3917.3	S?	605854	5581265	6.1	13.7	27.9	106.9	13.5	13.9	0.5	4	1122
L	3935.7	S	605852	5581678	2.3	19.5	8.6	91.0	14.5	8.7	---	---	0
M	3957.6	S?	605852	5582193	0.0	61.3	*	343.4	6.7	59.5	---	---	0
LINE 10100		FLIGHT 3											
A	4320.5	S	605943	5577854	16.3	29.5	108.0	154.2	11.3	34.7	0.8	0	0
B	4299.1	S?	605948	5578222	0.1	10.9	0.1	76.1	0.1	8.5	---	---	296
C	4294.1	S	605950	5578314	9.7	16.8	1.6	91.0	0.0	9.7	0.7	10	169
D	4275.5	B?	605930	5578638	67.4	108.3	389.8	575.3	21.2	135.0	1.5	0	0
E	4268.1	S?	605939	5578801	105.6	122.1	704.7	746.6	28.1	252.8	2.4	0	188
F	4264.9	E	605946	5578882	119.3	129.7	704.7	746.6	35.0	252.8	2.7	0	164
G	4248.4	S?	605956	5579233	11.4	33.4	63.9	192.5	7.6	32.3	0.5	0	0
H	4234.5	S	605943	5579605	10.5	10.6	41.1	27.2	5.1	10.2	1.3	10	0
I	4215.4	B?	605944	5580132	11.2	40.1	51.6	156.2	22.6	28.1	0.4	0	491
J	4191.0	S?	605946	5580792	2.7	30.8	32.7	259.8	0.1	36.6	---	---	1585
K	4160.7	S?	605944	5581334	2.5	33.6	16.6	289.8	0.2	32.8	---	---	0
L	4117.6	S?	605953	5581834	14.8	14.6	86.0	71.7	15.3	31.1	1.5	5	0
M	4102.3	S	605950	5582132	23.2	46.0	109.7	236.1	10.5	34.3	0.8	0	0
LINE 10110		FLIGHT 3											
A	4409.6	S	606044	5577619	1.8	11.7	16.0	77.2	6.6	10.4	---	---	0
B	4418.8	S	606045	5577934	15.2	24.9	65.6	108.2	13.5	18.4	0.9	10	0
C	4447.1	E	606055	5578689	22.2	53.0	109.2	556.6	8.5	126.1	0.7	0	174
D	4451.2	S?	606048	5578789	65.9	86.6	401.8	556.6	17.5	126.6	1.8	0	55
E	4470.6	S?	606044	5579251	12.4	57.6	91.5	342.9	15.1	49.9	0.3	0	0
F	4500.5	S	606046	5580016	6.0	10.3	43.1	116.6	5.3	18.0	0.6	22	0
G	4568.2	S	606049	5581416	3.1	14.0	17.1	91.5	0.8	12.0	0.2	0	371
H	4588.8	S?	606050	5581836	24.4	74.0	259.9	537.5	16.9	124.0	0.6	0	307
I	4603.7	S	606044	5582209	7.7	*	*	168.1	13.6	13.3	0.2	0	0
LINE 10120		FLIGHT 3											
A	4895.1	S	606145	5577907	5.5	13.4	49.2	74.1	17.7	14.1	0.5	8	49
B	4879.6	S?	606151	5578268	0.2	33.7	23.6	212.2	27.5	27.0	---	---	0
C	4843.9	S?	606150	5578858	41.4	72.2	297.1	518.6	22.5	98.8	1.2	0	175
D	4840.3	S	606154	5578947	30.4	51.3	297.1	518.6	22.5	98.8	1.1	6	0
E	4838.6	E	606156	5578986	30.4	24.0	297.1	61.0	28.2	98.8	2.5	14	66
F	4826.1	S?	606152	5579256	3.4	27.7	32.0	215.9	0.0	25.2	0.1	0	0
G	4816.5	S	606150	5579509	6.8	15.9	63.1	146.1	20.4	23.8	0.5	14	149

CX = COAXIAL
CP = COPLANAR

Note:EM values shown above are local amplitudes

*Estimated Depth may be unreliable because the stronger part of the conductor may be deeper or to one side of the flight line, or because of a shallow dip or magnetite/overburden effects

EM Anomaly List

Label	Fid	Interp	XUTM m	YUTM m	CX 5500 HZ Real ppm	CX 5500 HZ Quad ppm	CP 7200 HZ Real ppm	CP 7200 HZ Quad ppm	CP 900 HZ Real ppm	CP 900 HZ Quad ppm	Vertical Dike COND siemens	Vertical Dike DEPTH* m	Mag. Corr NT
LINE 10120		FLIGHT 3											
H	4738.8	S	606136	5581040	7.4	23.9	38.0	118.5	9.2	18.9	0.4	2	0
I	4719.8	S	606145	5581379	1.6	22.1	9.3	114.3	7.6	13.5	---	---	726
J	4695.8	E	606156	5581609	14.6	45.6	258.6	273.3	10.9	51.0	0.5	0	0
K	4689.9	S	606156	5581725	22.8	52.0	267.4	383.0	10.9	98.8	0.8	0	687
L	4685.8	S?	606157	5581821	9.9	46.8	267.4	272.8	53.9	80.4	0.3	0	650
M	4677.4	S?	606158	5582004	17.5	112.9	240.8	650.8	50.4	133.4	0.3	0	267
LINE 10130		FLIGHT 3											
A	4994.4	S?	606249	5577947	3.3	7.9	9.1	67.7	13.5	9.9	---	---	763
B	5024.7	S	606251	5578883	28.3	32.7	218.8	251.5	11.8	60.4	1.6	1	0
C	5026.7	S?	606251	5578951	29.6	53.5	218.8	251.5	11.8	60.4	1.0	2	427
D	5035.5	S?	606249	5579250	6.4	56.2	23.6	252.8	3.4	34.8	0.2	0	0
E	5048.9	S	606260	5579726	6.4	16.8	36.5	105.4	7.4	16.1	0.4	9	143
F	5070.8	S	606257	5580276	5.4	15.3	39.2	87.1	4.0	13.9	0.4	10	0
LINE 10131		FLIGHT 5											
A	3390.2	H	606238	5581187	10.7	5.8	48.1	32.3	24.6	9.8	2.8	21	0
B	3372.8	S?	606248	5581465	0.0	10.3	34.1	87.4	35.5	8.1	---	---	488
C	3346.5	S?	606250	5581688	28.3	94.4	289.4	528.6	22.1	119.2	0.6	0	538
D	3344.6	S	606250	5581729	28.3	94.4	289.4	528.6	22.1	119.2	0.6	0	538
E	3334.7	S	606250	5581940	12.2	29.3	232.6	346.5	5.3	84.8	0.6	1	149
LINE 10140		FLIGHT 3											
A	5573.2	S	606348	5577453	*	4.8	*	*	*	*	---	---	0
B	5545.9	S?	606365	5578073	2.4	15.2	22.7	132.4	41.8	18.0	---	---	1438
C	5540.6	S?	606361	5578176	1.9	8.8	8.9	119.8	9.3	16.0	---	---	0
D	5499.3	S?	606353	5578976	9.4	24.3	72.0	147.7	18.5	26.2	0.5	4	534
E	5488.5	S?	606344	5579228	1.7	18.5	18.3	125.6	6.4	19.6	---	---	0
F	5460.1	S	606347	5579812	4.3	7.6	43.7	81.3	16.6	12.8	0.5	32	0
G	5407.9	S?	606346	5580766	1.1	10.8	17.2	54.4	8.6	8.2	---	---	136
H	5397.5	S?	606343	5580921	0.1	10.5	6.7	78.1	7.5	9.7	---	---	0
I	5370.7	H	606342	5581217	6.2	1.7	57.8	25.0	13.3	16.6	---	---	0
J	5335.6	S	606355	5581746	20.4	49.3	265.5	375.7	56.6	106.2	0.7	0	0
K	5332.4	S	606355	5581819	9.8	14.1	200.2	375.7	65.5	69.4	0.9	17	0
L	5324.1	S?	606351	5581983	29.1	68.9	200.2	348.6	65.5	44.9	0.8	0	218
M	5316.6	S	606347	5582125	10.0	18.6	169.1	432.4	3.7	66.8	0.7	7	0
N	5313.4	E	606351	5582184	13.7	67.2	150.4	432.4	3.7	66.8	0.3	0	0

CX = COAXIAL
CP = COPLANAR

Note: EM values shown above are local amplitudes

*Estimated Depth may be unreliable because the stronger part of the conductor may be deeper or to one side of the flight line, or because of a shallow dip or magnetite/overburden effects

EM Anomaly List

Label	Fid	Interp	XUTM m	YUTM m	CX 5500 HZ Real ppm	CX 5500 HZ Quad ppm	CP 7200 HZ Real ppm	CP 7200 HZ Quad ppm	CP 900 HZ Real ppm	CP 900 HZ Quad ppm	Vertical Dike COND siemens	Vertical Dike DEPTH* m	Mag. Corr NT
LINE 10150			FLIGHT 3										
A	5654.6	S?	606459	5577625	5.0	15.0	34.6	105.7	23.7	11.8	0.4	11	195
B	5674.8	S?	606441	5578036	3.3	18.6	45.8	131.1	49.2	18.2	---	---	1135
C	5708.4	S	606456	5579129	5.9	9.7	26.2	81.1	8.0	14.3	---	---	116
D	5723.2	S?	606452	5579647	4.6	28.5	27.3	205.6	10.6	26.6	0.2	0	615
E	5729.8	S	606455	5579870	7.5	49.2	65.7	268.0	13.4	37.0	0.2	0	0
F	5749.0	S	606448	5580349	3.2	7.9	35.2	65.6	4.9	12.0	0.4	18	0
G	5771.8	S?	606447	5580728	2.0	6.0	25.2	60.9	20.4	9.2	---	---	0
H	5792.7	H	606451	5581199	1.9	6.4	56.5	54.4	4.5	15.6	---	---	53
I	5803.2	S	606447	5581435	9.2	13.8	83.2	91.7	6.7	29.4	0.8	1	0
J	5806.4	S?	606447	5581505	11.7	12.5	83.2	91.7	6.7	29.4	1.3	22	0
K	5817.5	S?	606450	5581719	6.0	27.8	75.9	197.5	12.9	36.6	0.3	0	0
L	5824.7	S?	606450	5581892	34.2	49.5	199.5	323.1	14.7	68.5	1.3	0	68
M	5828.5	E	606447	5581991	8.5	66.1	52.2	323.1	49.3	65.3	0.2	0	21
LINE 10160			FLIGHT 3										
A	6149.6	S	606553	5577441	6.9	*	37.1	*	23.4	*	0.2	0	0
B	6130.0	S	606549	5577911	8.1	11.0	36.9	121.8	37.5	15.8	---	---	0
C	6113.2	S	606554	5578227	10.6	18.3	89.9	108.6	51.7	20.2	0.7	10	0
D	6084.0	S?	606549	5578818	2.3	29.3	36.0	136.3	0.0	19.5	---	---	0
E	6074.5	B?	606540	5578972	8.5	14.1	11.9	15.4	14.9	1.2	0.7	15	313
F	6055.0	S	606554	5579330	3.0	13.0	35.8	85.4	3.1	14.1	---	---	0
G	6025.7	S	606542	5579956	7.4	39.0	36.8	170.8	7.9	22.6	0.3	0	0
H	5991.1	S	606548	5580684	1.5	1.8	28.1	34.2	28.1	5.9	---	---	0
I	5963.9	S	606551	5581071	12.3	22.6	97.6	125.6	13.8	27.9	0.7	9	0
J	5936.8	S	606554	5581555	5.1	13.2	34.5	61.2	11.0	9.6	0.4	9	0
K	5914.3	S	606548	5581910	22.1	59.6	118.0	353.9	21.7	46.9	0.7	0	0
LINE 10170			FLIGHT 3										
A	6286.5	S	606650	5578930	7.1	15.3	17.8	52.0	5.7	6.6	0.5	3	0
B	6308.6	S?	606650	5579552	3.1	9.6	15.9	88.6	0.0	11.7	---	---	0
C	6325.8	S	606657	5579886	4.4	21.1	34.9	152.5	26.7	20.5	0.2	0	0
D	6332.0	S?	606658	5580016	0.0	57.1	31.5	315.0	4.9	39.7	---	---	0
E	6366.9	S?	606642	5580791	1.6	13.0	8.0	49.7	6.4	4.8	---	---	166
F	6376.0	S	606644	5581033	3.1	6.1	34.1	22.6	14.1	7.2	---	---	0
G	6395.0	S	606651	5581564	6.5	16.6	21.8	80.3	4.8	10.6	0.5	2	0
H	6413.4	S?	606651	5581858	9.1	23.9	25.2	116.5	7.5	15.3	0.5	0	0

CX = COAXIAL
CP = COPLANAR

Note: EM values shown above are local amplitudes

*Estimated Depth may be unreliable because the stronger part of the conductor may be deeper or to one side of the flight line, or because of a shallow dip or magnetite/overburden effects

EM Anomaly List

Label	Fid	Interp	XUTM m	YUTM m	CX 5500 HZ Real ppm	CX 5500 HZ Quad ppm	CP 7200 HZ Real ppm	CP 7200 HZ Quad ppm	CP 900 HZ Real ppm	CP 900 HZ Quad ppm	Vertical Dike COND siemens	Vertical Dike DEPTH* m	Mag. Corr NT
LINE 10180			FLIGHT 3										
A	6822.6	S	606762	5578025	3.6	12.7	30.5	113.2	12.6	16.5	0.3	5	0
B	6786.0	S	606742	5578751	2.6	6.3	36.2	128.4	9.7	16.7	---	---	134
C	6761.7	S	606744	5579208	10.1	10.8	36.1	16.0	14.6	6.2	1.2	13	0
D	6739.9	S?	606745	5579569	1.1	16.7	12.1	106.1	0.0	12.7	---	---	0
E	6732.1	S	606748	5579657	3.4	0.0	15.5	1.6	24.3	0.2	---	---	0
F	6719.6	S?	606745	5579789	1.9	15.9	25.7	72.0	26.0	10.2	---	---	0
G	6708.6	S?	606747	5579958	15.1	16.8	38.0	79.9	31.3	8.2	1.3	2	0
H	6699.7	E	606737	5580128	0.7	11.5	11.2	70.1	21.5	10.4	---	---	1324
I	6651.0	S	606749	5581063	4.6	4.5	28.6	55.4	21.3	11.0	---	---	13
LINE 10190			FLIGHT 3										
A	7614.5	S	606852	5577992	3.0	11.1	44.3	97.5	17.3	17.6	0.3	5	0
B	7641.4	S?	606859	5578592	15.3	21.4	77.8	84.9	23.9	15.2	1.0	10	0
C	7652.6	S	606855	5578884	9.2	13.3	29.9	82.4	4.3	13.9	0.8	8	0
D	7663.8	E	606855	5579201	12.9	13.0	56.3	72.4	10.4	13.7	1.4	11	0
E	7708.5	S?	606851	5580010	22.5	78.3	116.4	492.8	0.0	67.4	0.5	0	0
F	7794.1	S	606858	5582148	5.1	14.1	12.0	69.5	4.3	10.7	0.4	3	0
LINE 10200			FLIGHT 3										
A	8120.7	S?	606952	5577866	1.0	8.8	7.1	45.1	18.5	6.5	---	---	787
B	8096.2	S	606953	5578386	4.7	13.5	14.8	55.9	9.6	5.7	0.4	13	0
C	8082.5	S?	606941	5578637	24.5	33.2	103.0	146.2	18.8	27.0	1.2	7	45
D	8065.1	S	606945	5579093	18.1	54.7	253.0	361.8	20.8	72.8	0.6	0	0
E	8062.2	S?	606947	5579170	33.1	46.3	253.0	361.8	20.8	72.8	1.3	0	0
F	8033.4	S	606957	5579577	7.5	17.1	37.4	114.3	18.8	17.2	0.5	8	0
G	8003.0	S	606946	5580025	5.3	17.0	51.2	115.3	2.1	21.5	0.4	4	0
H	7985.5	S?	606946	5580328	11.9	70.7	126.3	512.0	32.4	73.8	0.3	0	0
I	7974.2	E	606945	5580554	12.9	29.9	124.1	233.1	16.3	37.9	0.6	11	366
LINE 10210			FLIGHT 3										
A	8194.4	S	607058	5577479	7.3	22.8	67.5	104.4	7.5	18.9	0.4	0	0
B	8213.4	S?	607048	5577947	0.1	14.6	0.3	153.3	0.0	22.1	---	---	0
C	8251.0	S	607050	5578857	6.0	22.7	71.6	118.0	9.2	19.6	0.3	0	72
D	8258.3	S?	607051	5579088	0.0	16.0	72.6	141.3	10.4	29.7	---	---	249
E	8318.6	S	607056	5580229	5.4	7.4	51.5	89.2	8.5	15.1	0.8	20	0
F	8331.1	S	607059	5580495	4.8	12.9	81.7	144.8	4.4	30.5	0.4	0	0

CX = COAXIAL
CP = COPLANAR

Note: EM values shown above are local amplitudes

*Estimated Depth may be unreliable because the stronger part of the conductor may be deeper or to one side of the flight line, or because of a shallow dip or magnetite/overburden effects

EM Anomaly List

Label	Fid	Interp	XUTM m	YUTM m	CX 5500 HZ Real ppm	CX 5500 HZ Quad ppm	CP 7200 HZ Real ppm	CP 7200 HZ Quad ppm	CP 900 HZ Real ppm	CP 900 HZ Quad ppm	Vertical Dike COND siemens	Vertical Dike DEPTH* m	Mag. Corr NT
LINE 10220			FLIGHT 3										
A	8701.7	S	607154	5577509	6.8	18.4	*	*	44.6	*	0.4	0	0
B	8683.7	S	607157	5578052	2.3	16.1	23.4	122.6	2.5	18.8	---	---	884
C	8651.5	S	607158	5578791	8.0	25.2	95.4	171.2	25.1	27.6	0.4	0	0
D	8634.7	S?	607157	5579202	4.4	16.3	9.9	82.5	4.7	13.3	0.3	2	205
E	8615.6	S	607144	5579515	13.7	25.0	71.4	172.1	31.6	21.1	0.8	9	0
F	8600.2	E	607138	5579703	7.0	33.3	16.7	225.7	69.1	30.9	0.3	2	0
G	8596.8	S	607140	5579737	10.4	31.5	16.7	225.7	5.4	30.9	0.5	4	0
H	8569.0	S	607146	5580147	11.5	21.1	163.8	141.2	27.1	39.9	0.7	26	0
I	8559.3	S?	607146	5580340	2.4	24.7	81.1	352.2	21.5	59.9	---	---	25
J	8554.9	S?	607150	5580421	10.3	61.0	81.1	352.2	0.0	59.9	0.3	0	62
K	8515.1	S?	607146	5581203	3.0	55.6	38.7	384.0	0.0	49.9	0.1	0	0
LINE 10230			FLIGHT 3										
A	8917.4	S	607253	5577618	3.1	8.0	21.0	77.8	2.0	11.0	0.4	15	226
B	8930.4	E	607263	5577920	3.5	15.9	27.4	129.9	34.2	16.5	0.2	0	602
C	8941.0	S?	607255	5578096	2.7	6.6	39.4	56.8	39.6	7.5	---	---	31
D	8975.1	S	607253	5578805	1.5	7.4	30.1	54.4	12.1	9.5	---	---	45
E	8996.0	S	607253	5579297	4.1	15.6	37.7	113.0	2.1	19.3	0.3	1	0
F	9000.0	S?	607253	5579384	2.7	21.1	37.7	113.0	2.1	19.3	---	---	0
G	9014.3	S?	607258	5579669	6.5	10.9	6.7	60.6	1.2	6.7	0.6	16	0
H	9036.6	S	607252	5580073	23.1	25.8	148.7	222.4	4.7	45.3	1.5	5	0
I	9045.0	S	607244	5580304	9.4	31.5	99.8	250.6	0.5	39.7	0.4	0	0
J	9069.0	S	607250	5580975	6.2	19.2	57.9	108.0	10.7	14.1	0.4	15	0
K	9095.7	S	607258	5581680	4.7	7.1	21.3	42.3	5.9	7.5	---	---	0
LINE 10240			FLIGHT 3										
A	9413.8	S?	607351	5577972	1.8	10.9	10.1	59.8	14.0	7.1	---	---	0
B	9364.3	S	607363	5579170	2.7	9.4	29.4	42.1	7.8	9.6	---	---	167
C	9326.4	S?	607345	5579733	4.2	5.0	21.7	91.2	15.8	11.8	0.8	45	0
D	9304.2	S?	607353	5580108	11.4	17.5	99.6	132.8	18.3	23.4	0.9	19	0
E	9292.9	S?	607352	5580347	2.6	17.9	89.6	188.4	9.9	29.0	---	---	100
F	9283.6	S	607353	5580562	15.4	27.0	96.1	170.0	12.7	31.2	0.8	3	0
G	9259.7	S	607351	5580991	5.2	7.7	131.6	161.5	94.0	22.3	0.7	23	0
H	9254.4	S?	607348	5581090	25.0	30.5	127.2	161.5	92.5	22.3	1.4	9	1926
I	9208.3	S	607358	5581888	6.1	11.8	35.9	72.9	3.2	11.8	0.6	10	0

CX = COAXIAL
CP = COPLANAR

Note:EM values shown above are local amplitudes

*Estimated Depth may be unreliable because the stronger part of the conductor may be deeper or to one side of the flight line, or because of a shallow dip or magnetite/overburden effects

EM Anomaly List

Label	Fid	Interp	XUTM m	YUTM m	CX 5500 HZ Real ppm	CX 5500 HZ Quad ppm	CP 7200 HZ Real ppm	CP 7200 HZ Quad ppm	CP 900 HZ Real ppm	CP 900 HZ Quad ppm	Vertical Dike COND siemens	Vertical Dike DEPTH* m	Mag. Corr NT
LINE 10250			FLIGHT 3										
A	9552.3	S?	607449	5578369	1.8	5.4	4.5	83.5	5.7	8.8	---	---	763
LINE 10251			FLIGHT 5										
A	3047.8	S	607450	5579172	4.8	8.9	26.2	62.5	7.9	10.9	0.5	12	80
B	3016.5	S?	607436	5579574	0.6	10.8	14.8	76.6	32.7	9.6	---	---	0
C	2984.7	S?	607433	5579717	0.6	34.1	107.1	222.3	123.5	26.4	---	---	0
D	2971.8	S	607438	5579784	10.0	9.7	50.9	105.1	61.2	11.2	1.3	31	0
E	2956.1	S?	607433	5579942	3.5	21.6	20.0	42.3	10.3	10.7	0.2	0	0
LINE 10252			FLIGHT 3										
A	9631.7	S	607441	5580127	7.4	18.4	61.0	126.8	4.3	20.1	0.5	3	0
B	9666.7	S	607462	5580923	4.3	10.9	92.8	83.1	51.9	10.2	---	---	0
C	9677.4	S?	607454	5581186	0.0	17.0	0.0	95.9	0.0	10.4	---	---	1473
D	9712.1	S	607447	5581998	1.6	8.4	30.3	66.4	6.8	5.8	---	---	0
LINE 10260			FLIGHT 3										
A	9976.1	S	607551	5579138	4.9	3.0	45.9	81.4	5.6	14.0	---	---	61
B	9972.3	S	607552	5579230	6.6	17.4	45.9	89.4	24.9	14.0	0.4	4	61
C	9946.1	E	607557	5579564	1.5	10.7	21.8	72.6	13.4	11.5	---	---	0
D	9901.9	S	607548	5580334	3.1	11.9	32.5	92.0	1.7	14.2	0.3	4	0
E	9866.6	S	607552	5580939	11.1	30.0	57.7	151.5	24.1	19.3	0.5	0	52
LINE 10270			FLIGHT 3										
A	10190.0	S?	607647	5579025	0.0	13.1	7.0	60.5	12.9	8.6	---	---	331
B	10198.3	S	607654	5579262	5.6	13.7	39.2	95.6	39.3	12.5	0.5	10	605
C	10225.4	S?	607663	5579699	4.0	17.7	16.8	84.5	21.5	10.4	0.2	0	289
D	10244.2	S	607647	5579978	4.4	23.4	45.6	143.0	10.0	21.1	0.2	0	160
E	10264.5	B?	607649	5580328	11.4	38.7	26.3	119.0	4.8	14.9	0.4	1	0
F	10283.7	S	607665	5580649	3.9	8.8	15.9	18.7	21.9	1.5	0.4	17	0
G	10305.2	S	607648	5581090	2.1	21.3	18.1	150.5	1.1	20.1	---	---	327
LINE 10271			FLIGHT 5										
A	2665.6	S	607637	5580878	7.8	25.4	22.6	120.3	*	14.8	0.4	0	0
B	2652.7	S	607646	5581075	4.5	29.3	25.5	190.4	2.8	27.1	0.2	0	108
C	2597.6	S	607647	5581752	8.2	39.2	37.6	198.2	15.2	28.0	0.3	0	452

CX = COAXIAL
CP = COPLANAR

Note:EM values shown above are local amplitudes

*Estimated Depth may be unreliable because the stronger part of the conductor may be deeper or to one side of the flight line, or because of a shallow dip or magnetite/overburden effects

EM Anomaly List

Label	Fid	Interp	XUTM m	YUTM m	CX 5500 HZ Real ppm	CX 5500 HZ Quad ppm	CP 7200 HZ Real ppm	CP 7200 HZ Quad ppm	CP 900 HZ Real ppm	CP 900 HZ Quad ppm	Vertical Dike COND siemens	Vertical Dike DEPTH* m	Mag. Corr NT
LINE 10272		FLIGHT 3											
A	10339.9	S	607655	5581724	6.4	32.0	27.6	157.1	3.2	22.4	0.3	0	0
B	10360.9	S	607652	5582190	8.6	35.5	83.5	171.4	*	32.9	0.3	16	0
LINE 10280		FLIGHT 3											
A	10623.6	S?	607753	5578782	0.6	9.5	4.0	67.1	8.4	9.4	---	---	0
B	10600.3	S?	607758	5579255	1.1	16.7	10.3	83.5	8.1	11.9	---	---	586
C	10573.6	S	607746	5579691	3.1	14.8	30.0	114.0	9.4	16.6	0.2	0	318
D	10556.4	S	607746	5580014	3.0	10.7	13.2	67.6	1.0	8.6	---	---	0
E	10541.5	S	607752	5580305	3.7	21.7	20.8	109.3	4.4	15.4	0.2	0	388
F	10527.7	S	607747	5580539	1.4	12.9	39.0	123.5	4.6	16.6	---	---	0
G	10519.5	S	607752	5580729	4.4	9.8	39.0	44.1	11.5	15.8	---	---	0
H	10476.0	S?	607751	5581438	3.8	11.5	12.1	62.0	23.0	7.4	0.3	12	0
I	10450.6	S?	607760	5581759	0.3	17.6	20.1	104.8	32.3	15.8	---	---	227
LINE 10290		FLIGHT 3											
A	10734.8	S	607851	5578690	1.4	7.2	27.2	152.8	2.5	19.4	---	---	0
B	10810.1	S?	607851	5580285	2.7	27.2	64.7	114.9	8.0	14.7	---	---	0
LINE 10300		FLIGHT 3											
A	11131.5	S?	607950	5578749	0.0	12.4	1.2	86.2	32.1	11.1	---	---	0
B	11048.1	S?	607944	5580329	5.6	21.8	38.5	103.1	17.6	13.1	0.3	1	326
LINE 10310		FLIGHT 4											
A	863.0	S?	608052	5578742	2.2	20.4	2.6	81.3	0.8	10.7	---	---	146
B	878.6	S?	608066	5578954	1.8	15.8	15.7	83.6	10.6	14.8	---	---	91
C	899.5	S?	608044	5579333	5.2	11.2	16.2	73.8	10.3	12.6	0.5	17	172
D	956.7	S?	608045	5580276	8.8	25.1	37.2	87.0	10.0	9.1	0.5	1	0
E	976.2	B?	608054	5580671	6.6	12.0	12.0	46.0	15.9	7.0	0.6	14	0
LINE 10321		FLIGHT 5											
A	1669.6	S	608163	5579094	7.1	21.8	45.3	77.7	15.2	15.0	0.4	4	0
B	1658.4	S?	608159	5579323	2.3	32.6	17.7	123.0	8.9	20.7	---	---	52
C	1599.7	S?	608139	5580159	1.1	14.6	43.0	104.8	25.4	14.5	---	---	0
D	1595.1	S	608136	5580219	6.6	7.2	43.0	104.8	22.7	14.5	---	---	164
E	1469.4	S	608159	5581895	9.0	19.3	45.9	137.7	0.2	19.9	0.6	4	28

CX = COAXIAL
CP = COPLANAR

Note:EM values shown above are local amplitudes

*Estimated Depth may be unreliable because the stronger part of the conductor may be deeper or to one side of the flight line, or because of a shallow dip or magnetite/overburden effects

EM Anomaly List

Label	Fid	Interp	XUTM m	YUTM m	CX 5500 HZ Real ppm	CX 5500 HZ Quad ppm	CP 7200 HZ Real ppm	CP 7200 HZ Quad ppm	CP 900 HZ Real ppm	CP 900 HZ Quad ppm	Vertical Dike COND siemens	Vertical Dike DEPTH* m	Mag. Corr NT
LINE 10330			FLIGHT 4										
A	1589.6	S	608248	5578726	3.9	22.9	15.5	90.6	0.2	9.1	0.2	0	0
B	1601.9	S	608253	5578856	0.3	23.6	11.0	50.1	6.1	8.9	---	---	263
C	1615.7	S?	608257	5579011	14.5	18.5	47.3	48.3	12.2	8.6	1.1	13	0
D	1622.4	H	608261	5579127	0.0	4.6	47.3	48.3	11.7	9.4	---	---	0
E	1697.1	S	608251	5580232	8.9	18.6	41.7	57.4	28.0	7.4	0.6	4	0
F	1712.0	S?	608249	5580506	2.1	16.2	15.5	92.1	26.2	10.6	---	---	136
G	1725.0	H	608258	5580718	6.1	11.6	25.4	44.0	17.6	0.8	0.6	4	0
LINE 10331			FLIGHT 5										
A	2419.5	S	608248	5581338	9.2	24.4	70.1	183.8	0.9	29.8	0.5	2	0
B	2390.7	S	608255	5581822	4.2	10.7	37.9	92.4	1.4	16.0	0.4	13	0
C	2375.0	S	608237	5582129	11.2	35.4	44.2	177.6	2.7	23.9	0.5	0	0
LINE 10341			FLIGHT 5										
A	2086.1	S?	608367	5579019	5.0	6.0	29.5	21.1	1.3	4.7	---	---	0
B	2065.3	B?	608370	5579255	8.5	5.0	45.6	57.4	6.8	15.7	2.3	30	0
C	2045.9	E	608351	5579543	2.9	16.7	31.1	43.3	1.7	8.8	---	---	171
D	2042.9	S	608344	5579595	3.6	8.0	31.1	57.0	13.4	9.0	---	---	0
E	1993.5	S	608342	5580253	8.5	23.3	34.7	96.1	10.7	13.7	0.5	1	0
F	1962.8	S	608344	5580615	2.2	5.1	25.2	80.3	7.9	9.6	---	---	34
G	1916.4	S	608346	5581391	11.4	45.0	48.4	235.8	2.1	34.4	0.4	0	0
H	1899.3	S	608345	5581701	6.8	17.4	44.8	92.2	0.3	15.0	0.5	0	0
LINE 10350			FLIGHT 4										
A	2809.7	S?	608462	5578908	14.0	20.8	65.1	69.4	11.8	18.3	0.9	2	0
B	2813.9	E	608462	5578975	14.8	16.3	65.1	69.4	1.8	18.3	1.3	17	0
C	2831.2	S	608461	5579232	7.0	8.0	33.4	50.4	3.3	9.2	1.0	21	0
D	2866.6	S?	608438	5579669	1.8	12.8	0.0	136.3	0.0	15.7	---	---	386
E	2915.5	S?	608454	5580401	0.9	12.8	26.0	67.0	29.7	8.8	---	---	0
F	2980.6	B?	608440	5581663	10.6	29.6	23.4	94.1	3.0	12.1	0.5	1	0
G	2997.2	S	608443	5582030	3.2	15.4	27.1	64.4	1.6	9.9	0.2	0	0
LINE 10360			FLIGHT 4										
A	3301.5	S	608552	5578840	25.4	36.9	224.4	231.1	37.9	60.6	1.2	0	0
B	3295.6	E	608553	5578987	24.4	31.7	224.4	231.1	37.9	60.6	1.3	3	0
C	3275.7	S	608555	5579297	5.7	0.0	28.5	46.7	4.4	8.1	---	---	0
D	3245.3	S?	608543	5579791	0.0	14.4	9.0	60.7	4.3	6.8	---	---	429

CX = COAXIAL
CP = COPLANAR

Note:EM values shown above are local amplitudes

*Estimated Depth may be unreliable because the stronger part of the conductor may be deeper or to one side of the flight line, or because of a shallow dip or magnetite/overburden effects

EM Anomaly List

Label	Fid	Interp	XUTM m	YUTM m	CX 5500 HZ Real ppm	CX 5500 HZ Quad ppm	CP 7200 HZ Real ppm	CP 7200 HZ Quad ppm	CP 900 HZ Real ppm	CP 900 HZ Quad ppm	Vertical Dike COND siemens	Vertical Dike DEPTH* m	Mag. Corr NT
LINE 10360		FLIGHT 4											
E	3207.8	S?	608546	5580401	0.5	15.6	12.1	85.2	2.0	11.2	---	---	0
F	3186.2	S?	608557	5580736	0.3	8.6	0.5	56.7	4.7	7.7	---	---	0
G	3126.9	S	608541	5581634	2.5	14.1	29.2	89.8	2.5	13.6	---	---	37
H	3088.0	S?	608547	5582088	1.8	18.2	16.9	138.3	0.0	17.7	---	---	0
LINE 10371		FLIGHT 5											
A	3762.7	E	608640	5578735	7.6	25.3	31.4	181.7	9.2	34.6	0.4	0	0
B	3755.2	S?	608645	5578846	22.3	28.9	150.8	195.3	6.2	44.7	1.3	0	0
C	3751.2	S	608648	5578939	21.4	27.5	150.8	195.3	6.7	44.7	1.3	0	0
D	3749.4	E	608649	5578981	21.4	29.0	150.8	195.3	6.7	44.7	1.2	1	0
E	3720.1	S	608668	5579320	8.5	0.0	23.4	28.9	3.9	6.4	---	---	0
F	3669.6	S	608659	5579994	5.4	13.9	40.8	80.4	12.6	12.2	0.4	5	0
LINE 10372		FLIGHT 4											
A	3476.4	S	608646	5579984	2.2	13.7	58.2	66.9	25.1	10.5	---	---	32
B	3488.9	S	608657	5580241	1.3	4.5	2.3	0.1	2.0	0.0	---	---	0
C	3537.4	S	608642	5581130	7.6	34.7	47.3	197.8	7.6	27.0	0.3	0	0
D	3596.6	S?	608648	5582196	5.5	17.7	19.8	80.0	*	12.3	0.4	0	0
LINE 10380		FLIGHT 4											
A	3853.0	S	608744	5579030	10.0	14.0	50.0	83.7	1.6	14.7	0.9	19	51
B	3818.2	S?	608744	5579601	10.7	46.3	33.1	213.5	10.5	27.2	0.4	1	0
C	3798.3	S	608745	5579902	8.7	12.0	29.7	70.6	6.7	12.0	0.9	13	0
D	3782.9	S?	608752	5580197	0.0	14.0	6.1	86.1	1.5	11.9	---	---	0
E	3733.0	S	608750	5581105	6.0	17.4	38.6	135.6	6.0	19.1	0.4	0	109
F	3708.4	S	608757	5581629	1.2	15.7	21.7	92.4	10.0	13.3	---	---	316
LINE 10390		FLIGHT 4											
A	4077.5	S	608864	5578964	6.1	4.9	39.1	67.1	3.6	12.2	1.4	35	0
B	4122.1	S	608846	5579547	2.0	8.8	13.4	109.5	7.3	13.4	---	---	0
C	4129.5	S?	608843	5579616	0.4	11.7	15.1	132.9	1.3	15.9	---	---	0
D	4177.7	S	608852	5580402	4.5	9.8	23.5	41.6	4.7	7.7	---	---	11
E	4214.1	S	608839	5580996	7.0	16.0	24.1	81.3	7.8	12.3	0.5	0	0
F	4222.8	S	608857	5581183	7.2	16.6	17.3	68.0	6.7	10.0	0.5	7	0
G	4248.1	S	608858	5581658	0.5	7.5	4.1	53.6	4.5	6.8	---	---	314
LINE 10400		FLIGHT 4											
A	4597.6	S?	608949	5578802	3.0	8.5	26.6	70.7	2.6	11.4	---	---	0

CX = COAXIAL
CP = COPLANAR

Note:EM values shown above are local amplitudes

*Estimated Depth may be unreliable because the stronger part of the conductor may be deeper or to one side of the flight line, or because of a shallow dip or magnetite/overburden effects

EM Anomaly List

Label	Fid	Interp	XUTM m	YUTM m	CX 5500 HZ Real ppm	CX 5500 HZ Quad ppm	CP 7200 HZ Real ppm	CP 7200 HZ Quad ppm	CP 900 HZ Real ppm	CP 900 HZ Quad ppm	Vertical Dike COND siemens	Vertical Dike DEPTH* m	Mag. Corr NT
LINE 10400			FLIGHT 4										
B	4552.6	S	608957	5579282	9.2	14.6	32.3	69.7	2.1	11.8	0.8	11	0
C	4503.9	S	608950	5580074	4.3	15.0	38.9	60.2	15.1	11.0	0.3	0	0
D	4443.4	S	608944	5580992	2.1	2.9	26.2	19.4	10.1	5.2	---	---	0
LINE 10410			FLIGHT 4										
A	4684.6	S	609069	5578904	4.1	7.6	20.3	31.3	12.9	6.4	0.5	22	0
B	4696.1	S	609064	5579049	7.1	20.4	25.9	62.3	5.0	4.4	0.4	5	65
C	4719.3	S	609053	5579343	8.8	28.7	51.4	91.8	12.1	12.9	0.4	0	0
D	4770.4	S	609061	5579949	3.3	18.5	33.1	41.8	18.5	6.9	0.2	0	0
LINE 10411			FLIGHT 5										
A	947.3	S	609042	5580131	5.6	11.8	25.6	53.3	4.0	8.4	0.5	0	66
B	887.8	S	609057	5580732	2.6	22.8	15.5	82.6	3.7	12.4	---	---	76
C	874.7	S	609055	5580917	7.3	24.2	23.1	65.7	3.5	10.4	0.4	19	0
LINE 10412			FLIGHT 4										
A	4839.4	S	609044	5580785	1.3	6.5	15.7	66.7	1.6	10.1	---	---	0
B	4857.3	S	609032	5581077	7.3	27.5	42.7	125.8	5.1	18.0	0.3	0	0
C	4893.2	S	609058	5581552	5.3	12.3	22.1	92.9	14.3	12.2	---	---	47
D	4906.5	S	609061	5581750	5.8	12.8	17.3	93.4	10.4	12.0	0.5	14	0
LINE 10420			FLIGHT 4										
A	5178.7	S?	609166	5579719	5.4	7.6	15.5	40.8	11.3	5.0	---	---	0
B	5150.0	S	609140	5580136	0.0	8.7	12.4	50.6	3.7	6.1	---	---	0
C	5078.9	S	609137	5581035	4.7	8.0	42.2	66.2	5.3	9.3	0.6	25	0
D	5044.3	S	609150	5581508	4.1	13.3	22.3	77.4	9.2	10.4	0.3	7	0
E	5031.2	S	609151	5581786	2.8	14.9	22.6	94.8	8.9	12.8	---	---	148
LINE 10430			FLIGHT 4										
A	5446.4	S	609261	5578954	2.5	9.4	21.2	75.2	3.3	10.5	---	---	0
B	5469.5	B?	609266	5579291	3.5	5.1	22.0	35.1	4.6	3.6	---	---	0
C	5528.6	S?	609253	5580152	1.7	7.1	26.6	60.2	31.7	6.7	---	---	313
D	5558.4	S	609264	5580512	2.1	10.5	5.5	47.3	2.6	6.8	---	---	47
E	5569.2	S	609251	5580675	6.5	8.8	17.8	36.2	5.6	4.1	0.8	17	0
F	5595.2	S	609243	5581051	2.1	15.8	21.5	110.6	3.3	14.3	---	---	0
G	5623.7	S	609258	5581410	4.0	11.8	29.5	53.2	15.6	7.4	0.3	8	0
H	5652.9	S?	609253	5581943	0.0	13.6	25.0	85.4	15.1	11.1	---	---	158

CX = COAXIAL
CP = COPLANAR

Note: EM values shown above are local amplitudes

*Estimated Depth may be unreliable because the stronger part of the conductor may be deeper or to one side of the flight line, or because of a shallow dip or magnetite/overburden effects

EM Anomaly List

Label	Fid	Interp	XUTM m	YUTM m	CX 5500 HZ Real ppm	CX 5500 HZ Quad ppm	CP 7200 HZ Real ppm	CP 7200 HZ Quad ppm	CP 900 HZ Real ppm	CP 900 HZ Quad ppm	Vertical Dike COND siemens	Vertical Dike DEPTH* m	Mag. Corr NT
LINE 10440		FLIGHT 4											
A	5917.9	S	609350	5579552	9.4	11.7	64.1	57.3	26.7	11.9	1.0	15	0
B	5883.9	S?	609353	5580214	1.0	8.2	15.3	59.5	13.3	6.4	---	---	190
C	5823.0	S	609346	5580936	8.3	8.7	12.9	51.7	2.4	7.3	1.2	10	0
D	5782.7	S	609353	5581443	5.1	14.1	16.4	84.9	15.4	9.9	0.4	12	0
E	5763.2	S	609358	5581673	4.9	24.2	43.0	155.2	17.0	23.0	0.2	0	0
LINE 10450		FLIGHT 4											
A	6104.4	S	609459	5579601	5.7	9.0	31.8	58.8	5.1	9.9	0.7	19	0
B	6201.4	S	609447	5580924	5.6	11.8	8.9	49.4	4.8	6.4	0.5	0	0
C	6238.4	S	609456	5581366	4.0	8.1	17.7	63.0	7.8	9.0	---	---	0
D	6272.6	S?	609462	5581886	0.7	17.6	29.5	58.4	20.6	9.2	---	---	0
LINE 19010		FLIGHT 4											
A	6560.5	S?	605532	5582151	12.2	63.4	142.3	380.6	23.0	63.9	0.3	0	176
B	6548.0	S?	605829	5582150	14.7	28.5	197.1	419.3	8.8	73.9	0.7	0	0
C	6544.6	S?	605915	5582147	33.9	62.3	197.1	419.3	8.8	73.9	1.0	0	0
D	6539.2	B?	606057	5582145	7.6	17.6	55.1	129.1	8.0	25.2	0.5	3	0
E	6532.3	S	606231	5582144	13.7	11.3	74.7	2.5	14.4	8.6	1.8	20	0
F	6525.6	S?	606381	5582147	15.6	49.3	131.0	249.0	39.1	37.5	0.5	0	0
G	6503.8	S	606817	5582152	1.8	11.1	12.4	72.3	1.3	8.6	---	---	0
H	6474.5	S	607549	5582133	2.2	0.0	32.9	31.4	6.1	8.3	---	---	0
I	6468.7	S	607716	5582136	6.6	10.5	45.6	84.5	6.3	13.9	0.7	23	12
J	6450.7	S?	608206	5582149	15.8	75.0	154.3	523.7	9.9	75.2	0.4	0	0
K	6438.6	E	608528	5582141	10.7	26.1	70.7	189.7	4.6	33.4	0.6	4	0
LINE 19020		FLIGHT 4											
A	6744.9	S?	605284	5581023	12.4	97.3	152.1	473.4	36.7	75.2	0.2	0	0
B	6747.4	B?	605322	5581021	11.6	61.3	152.1	473.4	70.5	75.0	0.3	0	0
C	6758.0	E	605416	5581019	7.2	24.2	97.3	165.2	62.8	29.0	0.4	4	0
D	6814.0	B?	606524	5581024	6.6	6.4	21.3	23.2	5.0	5.7	---	---	0
E	6846.2	S	607170	5581021	0.5	3.4	21.1	74.8	3.7	8.2	---	---	0
F	6860.6	S?	607483	5581019	5.5	30.2	18.3	167.8	4.7	20.4	0.2	0	175
G	6874.8	S	607698	5581015	1.7	16.1	20.2	189.9	4.1	25.3	---	---	0
H	6929.9	S?	608702	5581024	8.1	19.6	47.4	199.5	41.2	24.7	0.5	9	0
LINE 19030		FLIGHT 4											
A	7289.8	S?	605393	5579892	49.3	71.3	265.9	404.0	22.5	78.8	1.5	0	0

CX = COAXIAL
CP = COPLANAR

Note:EM values shown above are local amplitudes

*Estimated Depth may be unreliable because the stronger part of the conductor may be deeper or to one side of the flight line, or because of a shallow dip or magnetite/overburden effects

EM Anomaly List

Label	Fid	Interp	XUTM m	YUTM m	CX 5500 HZ Real ppm	CX 5500 HZ Quad ppm	CP 7200 HZ Real ppm	CP 7200 HZ Quad ppm	CP 900 HZ Real ppm	CP 900 HZ Quad ppm	Vertical Dike COND siemens	Vertical Dike DEPTH* m	Mag. Corr NT
LINE 19030			FLIGHT 4										
B	7263.4	S	606002	5579913	13.5	16.2	58.1	102.4	8.3	18.8	1.2	3	77
C	7244.0	S	606492	5579908	8.3	31.0	67.9	209.0	11.4	25.8	0.4	0	0
D	7236.7	S?	606648	5579897	8.8	30.7	40.2	191.2	32.2	23.8	0.4	0	312
E	7221.7	S?	606960	5579908	4.8	22.4	42.5	142.2	14.8	20.7	0.3	2	0
F	7206.4	S	607244	5579916	10.8	20.9	52.1	117.4	7.6	18.0	0.7	27	235
G	7192.1	S?	607515	5579905	0.0	3.8	20.2	68.5	19.9	9.8	---	---	345
H	7181.7	S?	607692	5579909	4.3	12.9	23.5	118.7	16.7	15.2	---	---	0
I	7176.0	E	607794	5579912	3.5	5.9	22.3	118.7	19.8	15.2	---	---	47
J	7109.8	S	608733	5579898	5.1	19.7	35.7	135.2	8.2	18.2	0.3	6	0
LINE 19040			FLIGHT 4										
A	7391.4	S?	605024	5578793	7.9	34.0	72.1	337.7	24.3	48.5	0.3	3	0
B	7395.0	S?	605065	5578788	3.0	34.4	72.1	337.7	10.0	48.5	0.1	0	0
C	7411.9	S?	605219	5578771	0.8	3.6	0.0	98.3	4.4	6.7	---	---	0
D	7426.2	E	605457	5578762	30.7	35.3	236.6	140.1	40.4	65.7	1.6	0	0
E	7432.0	S?	605587	5578760	31.9	19.1	192.5	155.5	40.6	95.7	3.5	13	367
F	7439.2	S?	605773	5578764	61.9	27.4	291.6	109.5	83.0	91.0	6.5	0	0
G	7448.4	E	606037	5578770	68.0	60.1	368.2	374.9	18.8	112.8	2.8	0	0
H	7459.8	S?	606346	5578795	5.1	37.5	57.2	218.3	23.5	34.0	0.2	0	0
I	7473.2	S?	606550	5578789	0.9	15.4	0.3	82.7	0.1	9.8	---	---	33
J	7491.2	S	607001	5578786	16.0	34.4	96.2	202.5	9.1	35.9	0.7	6	0
K	7536.0	S?	607922	5578776	0.0	10.0	4.6	54.4	7.2	7.0	---	---	629
L	7562.7	S	608613	5578779	8.3	14.2	68.8	82.0	5.5	16.7	0.7	0	0
M	7597.3	S?	609221	5578781	5.2	20.9	27.4	107.3	9.3	14.5	0.3	0	0
LINE 19050			FLIGHT 4										
A	7881.0	S	604952	5577655	17.6	*	*	*	1.5	*	0.2	0	0
B	7862.2	S	605411	5577669	28.7	29.1	185.2	165.8	9.4	56.7	1.8	0	0
C	7856.5	S?	605555	5577670	30.9	45.5	145.1	126.1	9.4	40.1	1.2	0	0
D	7843.8	D	605863	5577673	29.2	106.5	129.5	472.2	2.4	83.0	0.6	0	0
E	7815.9	S?	606306	5577665	3.2	8.2	12.1	118.3	13.6	13.8	---	---	434
F	7804.9	S?	606463	5577665	1.1	16.5	33.0	127.5	10.5	15.4	---	---	0
G	7787.2	S	606820	5577670	5.2	5.5	44.7	73.7	1.7	14.9	1.0	41	0
H	7771.6	S	607187	5577653	6.4	24.2	53.0	166.1	2.8	26.2	0.3	0	248

CX = COAXIAL
CP = COPLANAR

Note:EM values shown above are local amplitudes

*Estimated Depth may be unreliable because the stronger part of the conductor may be deeper or to one side of the flight line, or because of a shallow dip or magnetite/overburden effects

APPENDIX F

GLOSSARY

APPENDIX F

GLOSSARY OF AIRBORNE GEOPHYSICAL TERMS

Note: The definitions given in this glossary refer to the common terminology as used in airborne geophysics.

altitude attenuation: the absorption of gamma rays by the atmosphere between the earth and the detector. The number of gamma rays detected by a system decreases as the altitude increases.

apparent- : the ***physical parameters*** of the earth measured by a geophysical system are normally expressed as apparent, as in "apparent ***resistivity***". This means that the measurement is limited by assumptions made about the geology in calculating the response measured by the geophysical system. Apparent resistivity calculated with ***HEM***, for example, generally assumes that the earth is a ***homogeneous half-space*** – not layered.

amplitude: The strength of the total electromagnetic field. In ***frequency domain*** it is most often the sum of the squares of ***in-phase*** and ***quadrature*** components. In multi-component electromagnetic surveys it is generally the sum of the squares of all three directional components.

analytic signal: The total amplitude of all the directions of magnetic ***gradient***. Calculated as the sum of the squares.

anisotropy: Having different ***physical parameters*** in different directions. This can be caused by layering or fabric in the geology. Note that a unit can be anisotropic, but still **homogeneous**.

anomaly: A localized change in the geophysical data characteristic of a discrete source, such as a conductive or magnetic body. Something locally different from the **background**.

B-field: In time-domain **electromagnetic** surveys, the magnetic field component of the (electromagnetic) **field**. This can be measured directly, although more commonly it is calculated by integrating the time rate of change of the magnetic field **dB/dt**, as measured with a receiver coil.

background: The "normal" response in the geophysical data – that response observed over most of the survey area. **Anomalies** are usually measured relative to the background. In airborne gamma-ray spectrometric surveys the term defines the **cosmic**, radon, and aircraft responses in the absence of a signal from the ground.

base-level: The measured values in a geophysical system in the absence of any outside signal. All geophysical data are measured relative to the system base level.

base frequency: The frequency of the pulse repetition for a ***time-domain electromagnetic*** system. Measured between subsequent positive pulses.

bird: A common name for the pod towed beneath or behind an aircraft, carrying the geophysical sensor array.

calibration coil: A wire coil of known size and dipole moment, which is used to generate a field of known ***amplitude*** and ***phase*** in the receiver, for system calibration. Calibration coils can be external, or internal to the system. Internal coils may be called Q-coils.

coaxial coils: **[CX]** Coaxial coils are in the vertical plane, with their axes horizontal and collinear in the flight direction. These are most sensitive to vertical conductive objects in the ground, such as thin, steeply dipping conductors perpendicular to the flight direction. Coaxial coils generally give the sharpest anomalies over localized conductors. (See also ***coplanar coils***)

coil: A multi-turn wire loop used to transmit or detect electromagnetic fields. Time varying ***electromagnetic*** fields through a coil induce a voltage proportional to the strength of the field and the rate of change over time.

compensation: Correction of airborne geophysical data for the changing effect of the aircraft. This process is generally used to correct data in ***fixed-wing time-domain electromagnetic*** surveys (where the transmitter is on the aircraft and the receiver is moving), and magnetic surveys (where the sensor is on the aircraft, turning in the earth's magnetic field.

component: In ***frequency domain electromagnetic*** surveys this is one of the two **phase** measurements – ***in-phase or quadrature***. In "multi-component" electromagnetic surveys it is also used to define the measurement in one geometric direction (vertical, horizontal in-line and horizontal transverse – the Z, X and Y components).

Compton scattering: gamma ray photons will bounce off the nuclei of atoms they pass through (earth and atmosphere), reducing their energy and then being detected by ***radiometric*** sensors at lower energy levels. See also ***stripping***.

conductance: See ***conductivity thickness***

conductivity: [σ] The facility with which the earth or a geological formation conducts electricity. Conductivity is usually measured in milli-Siemens per metre (mS/m). It is the reciprocal of ***resistivity***.

conductivity-depth imaging: see ***conductivity-depth transform***.

conductivity-depth transform: A process for converting electromagnetic measurements to an approximation of the conductivity distribution vertically in the earth, assuming a ***layered earth***. (Macnae and Lamontagne, 1987; Wolfgram and Karlik, 1995)

conductivity thickness: [σt] The product of the ***conductivity***, and thickness of a large, tabular body. (It is also called the "conductivity-thickness product") In electromagnetic geophysics, the response of a thin plate-like conductor is proportional to the conductivity multiplied by thickness. For example a 10 metre thickness of 20 Siemens/m mineralization will be equivalent to 5 metres of 40 S/m; both have 200 S conductivity thickness. Sometimes referred to as conductance.

conductor: Used to describe anything in the ground more conductive than the surrounding geology. Conductors are most often clays or graphite, or hopefully some type of mineralization, but may also be man-made objects, such as fences or pipelines.

coplanar coils: **[CP]** The coplanar coils lie in the horizontal plane with their axes vertical, and parallel. These coils are most sensitive to massive conductive bodies, horizontal layers, and the ***halfspace***.

cosmic ray: High energy sub-atomic particles from outer space that collide with the earth's atmosphere to produce a shower of gamma rays (and other particles) at high energies.

counts (per second): The number of ***gamma-rays*** detected by a gamma-ray ***spectrometer.*** The rate depends on the geology, but also on the size and sensitivity of the detector.

culture: A term commonly used to denote any man-made object that creates a geophysical anomaly. Includes, but not limited to, power lines, pipelines, fences, and buildings.

current gathering: The tendency of electrical currents in the ground to channel into a conductive formation. This is particularly noticeable at higher frequencies or early time channels when the formation is long and parallel to the direction of current flow. This tends to enhance anomalies relative to inductive currents (see also ***induction***). Also known as current channelling.

current channelling: See current gathering.

daughter products: The radioactive natural sources of gamma-rays decay from the original element (commonly potassium, uranium, and thorium) to one or more lower-energy elements. Some of these lower energy elements are also radioactive and decay further. ***Gamma-ray spectrometry*** surveys may measure the gamma rays given off by the original element or by the decay of the daughter products.

dB/dt: As the ***secondary electromagnetic field*** changes with time, the magnetic field [**B**] component induces a voltage in the receiving ***coil***, which is proportional to the rate of change of the magnetic field over time.

decay: In ***time-domain electromagnetic*** theory, the weakening over time of the ***eddy currents*** in the ground, and hence the ***secondary field*** after the ***primary field*** electromagnetic pulse is turned off. In ***gamma-ray spectrometry***, the radioactive breakdown of an element, generally potassium, uranium, thorium, or one of their ***daughter*** products.

decay series: In ***gamma-ray spectrometry***, a series of progressively lower energy ***daughter products*** produced by the radioactive breakdown of uranium or thorium.

decay constant: see time constant.

depth of exploration: The maximum depth at which the geophysical system can detect the target. The depth of exploration depends very strongly on the type and size of the target, the contrast of the target with the surrounding geology, the homogeneity of the surrounding geology, and the type of geophysical system. One measure of the maximum depth of exploration for an electromagnetic system is the depth at which it can detect the strongest conductive target – generally a highly conductive horizontal layer.

differential resistivity: A process of transforming ***apparent resistivity*** to an approximation of layer resistivity at each depth. The method uses multi-frequency HEM data and approximates the effect of shallow layer ***conductance*** determined from higher frequencies to estimate the deeper conductivities (Huang and Fraser, 1996)

dipole moment: [NIA] For a transmitter, the product of the area of a ***coil***, the number of turns of wire, and the current flowing in the coil. At a distance significantly larger than the size of the coil, the magnetic field from a coil will be the same if the dipole moment product is the same. For a receiver coil, this is the product of the area and the number of turns. The sensitivity to a magnetic field (assuming the source is far away) will be the same if the dipole moment is the same.

diurnal: The daily variation in a natural field, normally used to describe the natural fluctuations (over hours and days) of the earth's magnetic field.

dielectric permittivity: **[ε]** The capacity of a material to store electrical charge, this is most often measured as the relative permittivity [ε_r], or ratio of the material dielectric to that of free space. The effect of high permittivity may be seen in HEM data at high frequencies over highly resistive geology as a reduced or negative ***in-phase***, and higher ***quadrature*** data.

drift: Long-time variations in the base-level or calibration of an instrument.

eddy currents: The electrical currents induced in the ground, or other conductors, by a time-varying ***electromagnetic field*** (usually the ***primary field***). Eddy currents are also induced in the aircraft's metal frame and skin; a source of ***noise*** in EM surveys.

electromagnetic: **[EM]** Comprised of a time-varying electrical and magnetic field. Radio waves are common electromagnetic fields. In geophysics, an electromagnetic system is one which transmits a time-varying ***primary field*** to induce ***eddy currents*** in the ground, and then measures the ***secondary field*** emitted by those eddy currents.

energy window: A broad spectrum of ***gamma-ray*** energies measured by a spectrometric survey. The energy of each gamma-ray is measured and divided up into numerous discrete energy levels, called windows.

equivalent (thorium or uranium): The amount of radioelement calculated to be present, based on the gamma-rays measured from a **daughter** element. This assumes that the ***decay series*** is in equilibrium – progressing normally.

fiducial, or fid: Timing mark on a survey record. Originally these were timing marks on a profile or film; now the term is generally used to describe 1-second interval timing records in digital data, and on maps or profiles.

fixed-wing: Aircraft with wings, as opposed to "rotary wing" helicopters.

footprint: This is a measure of the area of sensitivity under the aircraft of an airborne geophysical system. The footprint of an ***electromagnetic*** system is dependent on the altitude of the system, the orientation of the transmitter and receiver and the separation between the receiver and transmitter, and the conductivity of the ground. The footprint of a ***gamma-ray spectrometer*** depends mostly on the altitude. For all geophysical systems, the footprint also depends on the strength of the contrasting ***anomaly***.

frequency domain: An ***electromagnetic*** system which transmits a ***primary field*** that oscillates smoothly over time (sinusoidal), inducing a similarly varying electrical current in the ground. These systems generally measure the changes in the ***amplitude*** and ***phase*** of the ***secondary field*** from the ground at different frequencies by measuring the **in-phase** and **quadrature** phase components. See also ***time-domain***.

full-stream data: Data collected and recorded continuously at the highest possible sampling rate. Normal data are stacked (see ***stacking***) over some time interval before recording.

gamma-ray: A very high-energy photon, emitted from the nucleus of an atom as it undergoes a change in energy levels.

gamma-ray spectrometry: Measurement of the number and energy of natural (and sometimes man-made) gamma-rays across a range of photon energies.

gradient: In magnetic surveys, the gradient is the change of the magnetic field over a distance, either vertically or horizontally in either of two directions. Gradient data is often measured, or calculated from the total magnetic field data because it changes more quickly over distance than the ***total magnetic field***, and so may provide a more precise measure of the location of a source. See also ***analytic signal***.

ground effect: The response from the earth. A common calibration procedure in many geophysical surveys is to fly to altitude high enough to be beyond any measurable response from the ground, and there establish ***base levels*** or ***backgrounds***.

half-space: A mathematical model used to describe the earth – as infinite in width, length, and depth below the surface. The most common halfspace models are ***homogeneous*** and ***layered earth***.

heading error: A slight change in the magnetic field measured when flying in opposite directions.

HEM: Helicopter ElectroMagnetic, This designation is most commonly used to helicopter-borne, ***frequency-domain*** electromagnetic systems. At present, the transmitter and receivers are normally mounted in a ***bird*** carried on a sling line beneath the helicopter.

herringbone pattern: a pattern created in geophysical data by an asymmetric system, where the **anomaly** may be extended to either side of the source, in the direction of flight. Appears like fish bones, or like the teeth of a comb, extending either side of centre, each tooth an alternate flight line.

homogeneous: This is a geological unit that has the same ***physical parameters*** throughout its volume. This unit will create the same response to an HEM system anywhere, and the HEM system will measure the same apparent ***resistivity*** anywhere. The response may change with system direction (see ***anisotropy***).

in-phase: the component of the measured ***secondary field*** that has the same phase as the transmitter and the ***primary field***. The in-phase component is stronger than the ***quadrature*** phase over relatively higher ***conductivity***.

induction: Any time-varying electromagnetic field will induce (cause) electrical currents to flow in any object with non-zero ***conductivity***. (see ***eddy currents***)

infinite: In geophysical terms, an "infinite' dimension is one much greater than the ***footprint*** of the system, so that the system does not detect changes at the edges of the object.

International Geomagnetic Reference Field: **[IGRF]** An approximation of the smooth magnetic field of the earth, in the absence of variations due to local geology. Once the IGRF is subtracted from the measured magnetic total field data, any remaining variations are assumed to be due to local geology. The IGRF also predicts the slow changes of the field up to five years in the future.

inversion, or **inverse modeling**: A process of converting geophysical data to an earth model, which compares theoretical models of the response of the earth to the data measured, and refines the model until the response closely fits the measured data (Huang and Palacky, 1991)

layered earth: A common geophysical model which assumes that the earth is horizontally layered – the ***physical parameters*** are constant to ***infinite*** distance horizontally, but change vertically.

magnetic permeability: **[μ]** This is defined as the ratio of magnetic induction to the inducing magnetic field. The relative magnetic permeability [μ_r] is often quoted, which is the ratio of the rock permeability to the permeability of free space. In geology and geophysics, the ***magnetic susceptibility*** is more commonly used to describe rocks.

magnetic susceptibility: **[k]** A measure of the degree to which a body is magnetized. In SI units this is related to relative ***magnetic permeability*** by $k=\mu_r-1$, and is a dimensionless unit. For most geological material, susceptibility is influenced primarily by the percentage of magnetite. It is most often quoted in units of 10^{-6}. In HEM data this is most often apparent as a negative ***in-phase*** component over high susceptibility, high ***resistivity*** geology such as diabase dikes.

noise: That part of a geophysical measurement that the user does not want. Typically this includes electronic interference from the system, the atmosphere (***sferics***), and man-made sources. This can be a subjective judgment, as it may include the response from geology other than the target of interest. Commonly the term is used to refer to high frequency (short period) interference. See also ***drift***.

Occam's inversion: an ***inversion*** process that matches the measured ***electromagnetic*** data to a theoretical model of many, thin layers with constant thickness and varying resistivity (Constable et al, 1987).

off-time: In a ***time-domain electromagnetic*** survey, the time after the end of the ***primary field pulse***, and before the start of the next pulse.

on-time: In a ***time-domain electromagnetic*** survey, the time during the ***primary field pulse***.

phase: The angular difference in time between a measured sinusoidal electromagnetic field and a reference – normally the primary field. The phase is calculated from $\tan^{-1}$(***in-phase / quadrature***).

physical parameters: These are the characteristics of a geological unit. For electromagnetic surveys, the important parameters for electromagnetic surveys are

conductivity, magnetic permeability (or ***susceptibility***) and ***dielectric permittivity***; for magnetic surveys the parameter is magnetic susceptibility, and for gamma ray spectrometric surveys it is the concentration of the major radioactive elements: potassium, uranium, and thorium.

permittivity: see ***dielectric permittivity.***

permeability: see ***magnetic permeability.***

primary field: the EM field emitted by a transmitter. This field induces ***eddy currents*** in (energizes) the conductors in the ground, which then create their own ***secondary*** **fields**.

pulse: In time-domain EM surveys, the short period of intense ***primary*** field transmission. Most measurements (the ***off-time***) are measured after the pulse.

quadrature: that component of the measured ***secondary field*** that is phase-shifted 90° from the ***primary field***. The quadrature component tends to be stronger than the ***in-phase*** over relatively weaker ***conductivity***.

Q-coils: see ***calibration coil.***

radiometric: Commonly used to refer to ***gamma ray*** spectrometry.

radon: A radioactive daughter product of uranium and thorium, radon is a gas which can leak into the atmosphere, adding to the non-geological background of a gamma-ray spectrometric survey.

resistivity: **[ρ]** The strength with which the earth or a geological formation resists the flow of electricity, typically the flow induced by the ***primary field*** of the electromagnetic transmitter. Normally expressed in ohm-metres, it is the reciprocal of ***conductivity.***

resistivity-depth transforms: similar to ***conductivity depth transforms***, but the calculated ***conductivity*** has been converted to ***resistivity***.

resistivity section: an approximate vertical section of the resistivity of the layers in the earth. The resistivities can be derived from the ***apparent resistivity***, the ***differential resistivities***, ***resistivity-depth transforms***, or ***inversions***.

secondary field: The field created by conductors in the ground, as a result of electrical currents induced by the ***primary field*** from the ***electromagnetic*** transmitter. Airborne ***electromagnetic*** systems are designed to create, and measure a secondary field.

Sengpiel section: a ***resistivity section*** derived using the ***apparent resistivity*** and an approximation of the depth of maximum sensitivity for each frequency.

sferic: Lightning, or the ***electromagnetic*** signal from lightning, it is an abbreviation of "atmospheric discharge". These appear to magnetic and electromagnetic sensors as sharp "spikes" in the data. Under some conditions lightning storms can be detected from hundreds of kilometres away. (see ***noise***)

signal: That component of a measurement that the user wants to see – the response from the targets, from the earth, etc. (See also ***noise***)

skin depth: A measure of the depth of penetration of an electromagnetic field into a material. It is defined as the depth at which the primary field decreases to 1/e of the field at the surface. It is calculated by approximately 503 x √(resistivity/frequency). Note that depth of penetration is greater at higher ***resistivity*** and/or lower ***frequency***.

spectrometry: Measurement across a range of energies, where ***amplitude*** and energy are defined for each measurement. In gamma-ray spectrometry, the number of gamma rays are measured for each energy ***window***, to define the ***spectrum***.

spectrum: In ***gamma ray spectrometry***, the continuous range of energy over which gamma rays are measured. In ***time-domain electromagnetic*** surveys, the spectrum is the energy of the **pulse** distributed across an equivalent, continuous range of frequencies.

spheric: see ***sferic***.

stacking: Summing repeat measurements over time to enhance the repeating ***signal***, and minimize the random ***noise***.

stripping: Estimation and correction for the gamma ray photons of higher and lower energy that are observed in a particular ***energy window***. See also ***Compton scattering***.

susceptibility: See ***magnetic susceptibility***.

tau: [τ] Often used as a name for the ***time constant***.

TDEM: ***time domain electromagnetic***.

thin sheet: A standard model for electromagnetic geophysical theory. It is usually defined as thin, flat-lying, and ***infinite*** in both horizontal directions. (see also ***vertical plate***)

tie-line: A survey line flown across most of the ***traverse lines***, generally perpendicular to them, to assist in measuring ***drift*** and ***diurnal*** variation. In the short time required to fly a tie-line it is assumed that the drift and/or diurnal will be minimal, or at least changing at a constant rate.

time constant: The time required for an ***electromagnetic*** field to decay to a value of 1/e of the original value. In ***time-domain*** electromagnetic data, the time constant is proportional to the size and ***conductance*** of a tabular conductive body. Also called the decay constant.

Time channel: In ***time-domain electromagnetic*** surveys the decaying ***secondary field*** is measured over a period of time, and the divided up into a series of consecutive discrete measurements over that time.

time-domain: ***Electromagnetic*** system which transmits a pulsed, or stepped ***electromagnetic*** field. These systems induce an electrical current (***eddy current***) in the ground that persists after the ***primary field*** is turned off, and measure the change over time of the ***secondary field*** created as the currents ***decay***. See also ***frequency-domain***.

total energy envelope: The sum of the squares of the three ***components*** of the ***time-domain electromagnetic secondary field***. Equivalent to the ***amplitude*** of the secondary field.

transient: Time-varying. Usually used to describe a very short period pulse of ***electromagnetic*** field.

traverse line: A normal geophysical survey line. Normally parallel traverse lines are flown across the property in spacing of 50 m to 500 m, and generally perpendicular to the target geology.

vertical plate: A standard model for electromagnetic geophysical theory. It is usually defined as thin, and ***infinite*** in horizontal dimension and depth extent. (see also ***thin sheet***)

waveform: The shape of the ***electromagnetic pulse*** from a ***time-domain*** electromagnetic transmitter.

window: A discrete portion of a ***gamma-ray spectrum*** or ***time-domain electromagnetic decay***. The continuous energy spectrum or ***full-stream*** data are grouped into windows to reduce the number of samples, and reduce ***noise***.

Version 1.1, March 10, 2003
Greg Hodges,
Chief Geophysicist
Fugro Airborne Surveys, Toronto

Common Symbols and Acronyms

k Magnetic susceptibility
ε Dielectric permittivity
μ, μ_r Magnetic permeability, apparent permeability
ρ, ρ_a Resistivity, apparent resistivity
σ,σ_a Conductivity, apparent conductivity
σt Conductivity thickness
τ Tau, or time constant
Ω.m Ohm-metres, units of resistivity
AGS Airborne gamma ray spectrometry.
CDT Conductivity-depth transform, conductivity-depth imaging (Macnae and Lamontagne, 1987; Wolfgram and Karlik, 1995)
CPI, CPQ Coplanar in-phase, quadrature
CPS Counts per second
CTP Conductivity thickness product
CXI, CXQ Coaxial, in-phase, quadrature
fT femtoteslas, normal unit for measurement of B-Field
EM Electromagnetic
keV kilo electron volts – a measure of gamma-ray energy
MeV mega electron volts – a measure of gamma-ray energy 1MeV = 1000keV
NIA dipole moment: turns x current x Area
nT nano-Tesla, a measure of the strength of a magnetic field
ppm parts per million – a measure of secondary field or noise relative to the primary.
pT/s picoTeslas per second: Units of decay of secondary field, dB/dt
S Siemens – a unit of conductance
x: the horizontal component of an EM field parallel to the direction of flight.
y: the horizontal component of an EM field perpendicular to the direction of flight.
z: the vertical component of an EM field.

References:

Constable, S.C., Parker, R.L., And Constable, C.G., 1987, Occam's inversion: a practical algorithm for generating smooth models from electromagnetic sounding data: Geophysics, 52, 289-300

Huang, H. and Fraser, D.C, 1996. The differential parameter method for muiltifrequency airborne resistivity mapping. Geophysics, 55, 1327-1337

Huang, H. and Palacky, G.J., 1991, Damped least-squares inversion of time-domain airborne EM data based on singular value decomposition: Geophysical Prospecting, v.39, 827-844

Macnae, J. and Lamontagne, Y., 1987, Imaging quasi-layered conductive structures by simple processing of transient electromagnetic data: Geophysics, v52, 4, 545-554.

Sengpiel, K-P. 1988, Approximate inversion of airborne EM data from a multi-layered ground. Geophysical Prospecting, 36, 446-459

Wolfgram, P. and Karlik, G., 1995, Conductivity-depth transform of GEOTEM data: Exploration Geophysics, 26, 179-185.

Yin, C. and Fraser, D.C. (2002), The effect of the electrical anisotropy on the responses of helicopter-borne frequency domain electromagnetic systems, Submitted to *Geophysical Prospecting*